DFG-Schwerpunktprogramm 1324

„Extraktion quantifizierbarer Information aus komplexen Systemen”

On the Butterfly Sparse Fourier Transform

S. Kunis, I. Melzer

Preprint 96

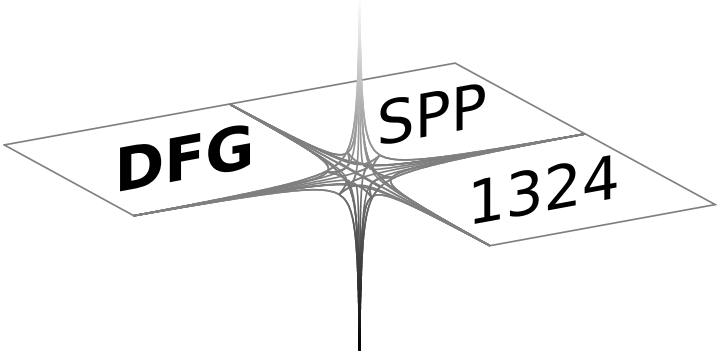

Edited by

AG Numerik/Optimierung
Fachbereich 12 - Mathematik und Informatik
Philipps-Universität Marburg
Hans-Meerwein-Str.
35032 Marburg

DFG-Schwerpunktprogramm 1324

„Extraktion quantifizierbarer Information aus komplexen Systemen”

On the Butterfly Sparse Fourier Transform

S. Kunis, I. Melzer

Preprint 96

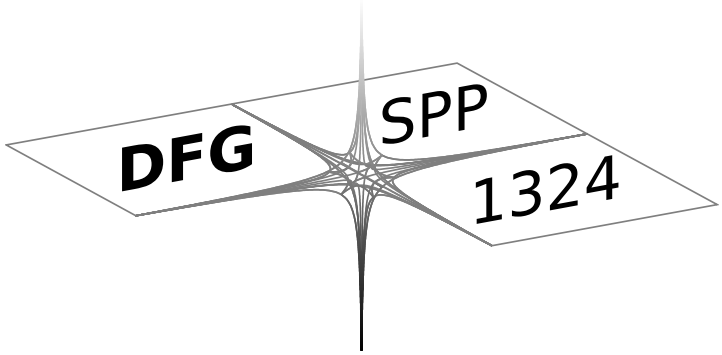

The consecutive numbering of the publications is determined by their chronological order.

The aim of this preprint series is to make new research rapidly available for scientific discussion. Therefore, the responsibility for the contents is solely due to the authors. The publications will be distributed by the authors.

On the butterfly sparse Fourier transform

Stefan Kunis[†] Ines Melzer[‡]

Recently, the butterfly approximation scheme has been proposed for computing Fourier transforms with sparse and smooth sampling in frequency and spatial domain. We present a rigorous error analysis which shows how the local expansion degree depends on the target accuracy and the nonharmonic bandwidth. Moreover, we show that the original scheme becomes numerically unstable if a large local expansion degree is used. This remedy is removed by representing all approximations in a Lagrange type basis instead of the previously used monomial basis. All theoretical results are illustrated by numerical experiments.

Key words and phrases : trigonometric approximation, nonharmonic Fourier series, fast Fourier transform.

2010 AMS Mathematics Subject Classification : 65T40, 65T50, 42A15.

1 Introduction

The fast Fourier transform (FFT) [3, 7] belongs to the algorithms with large impact on science and engineering. Shortcomings are the need for equispaced sampling and the fact that sparsity, as used in many recent approaches to tackle large scale and high dimensional problems, is not reflected in reduced computational costs.

The development of nonequispaced FFTs is well understood, see e.g. [9] and references therein, and the common concept in such schemes is to trade exactness for efficiency; instead of precise computations up to machine precision, the proposed methods guarantee a given target accuracy. In its most general form, given a space dimension $d \in \mathbb{N}$, a nonharmonic bandwidth $N = 2^L$, $L \in \mathbb{N}$, a set of frequencies $\tilde{T} = \{\boldsymbol{\xi}_k \in [0,N]^d : k = 1,\dots,M_2\}$, a set of Fourier coefficients $\hat{f}_k \in \mathbb{C}$, $k = 1,\dots,M_2$, and a set of evaluation nodes $\tilde{X} = \{\boldsymbol{x}_j \in [0,N]^d : j = 1,\dots,M_1\}$, we aim to compute the sums

$$u_j = u(\boldsymbol{x}_j) = \sum_{k=1}^{M_2} \hat{f}_k \mathrm{e}^{2\pi \mathrm{i} \boldsymbol{\xi}_k \boldsymbol{x}_j}, \quad j = 1,\dots,M_1. \tag{1.1}$$

While the naive computation takes $\mathcal{O}(M_1 M_2)$ floating point operations, the FFT for nonequispaced data in space and frequency domain [5] or type-3 nonuniform FFT [8] reduce this to $\mathcal{O}(N^d \log N + |\log \varepsilon|^d (M_1 + M_2))$, where $\varepsilon > 0$ denotes the target accuracy.

[†]University Osnabrück, Institute of Mathematics, and Helmholtz Zentrum München, Institute for Biomathematics and Biometry, stefan.kunis@math.uos.de

[‡]University Osnabrück, Institute of Mathematics, ines.melzer@uos.de

Within the area of analysis-based fast algorithms, these nonequispaced FFTs and fast multipole methods have recently become another cousin by the so-called butterfly approximation scheme, which can be traced back at least to [11] and has found a series of recent applications in [16, 12, 14]. Moreover it is well known that certain blocks of the discrete Fourier transform are approximately of low rank [4], which has lead to the butterfly sparse Fourier transforms [1, 15]. Hence, the sums (1.1) with $d \geq 2$, $M_1 = M_2 = \mathcal{O}(N^{d-1})$, and well distributed sampling sets $\tilde{T}, \tilde{X}$ on smooth $d-1$ dimensional manifolds, can be computed in $\mathcal{O}(N^{d-1} \log N p^{d+1})$ floating point operations, where $p \in \mathbb{N}$ denotes the local expansion degree.

In this paper, we follow [15] and present a rigorous error analysis which shows how the local expansion degree depends on the target accuracy and the nonharmonic bandwidth. After introducing the necessary notation and modifying the original approach slightly, we prove in Theorem 2.4 an error estimate given a local admissibility condition is fulfilled. The combination of the local approximation is done via the butterfly scheme in Section 3 and we prove how the error propagates through the different levels of the method in Theorem 3.1 - this also allows for a precise complexity estimate. Moreover, we show that the original scheme becomes numerically unstable if a large local expansion degree is used and remove this remedy by representing all approximations in a Lagrange type basis instead of the previously used monomial basis, cf. Section 2.3. All theoretical results are illustrated by numerical experiments and we finally conclude our findings in Section 5.

2 Local approximation

Let the numbers $p, N \in \mathbb{N}$, $p \geq 2$, be fixed and let the Chebyshev polynomials of the first kind $T_p : [-1,1] \to \mathbb{R}$, $T_p(x) = \cos(p \arccos x)$, be given. The zeros of the p-th Chebyshev polynomial are given by

$$t_j = \cos \frac{2j+1}{2p}\pi, \quad j = 0, \dots, p-1. \tag{2.1}$$

We call $A := [a,b]$, $a < b$, box and denote its width and its center by $w^A := \operatorname{diam} A = b - a$ and $c^A := \frac{a+b}{2}$, respectively. Further, we define in $\left[-\frac{1}{2}, \frac{1}{2}\right]$ the vector of the normalised Chebyshev nodes and the vector of the equispaced nodes by

$$\boldsymbol{\alpha} = (\alpha_j)_{j=0}^{p-1}, \ \alpha_j = \frac{1}{2} t_j, \quad \boldsymbol{\beta} = (\beta_j)_{j=0}^{p-1}, \ \beta_j = \frac{1}{2} - \frac{j}{p-1}.$$

For a box $B \subset \mathbb{R}$ we define the linear space of all finite expansions of exponential functions

$$\Pi_B(A) := \left\{ g : A \to \mathbb{C} : \exists K \in \mathbb{N} : g(x) = \sum_{j=1}^{K} c_j \mathrm{e}^{2\pi \mathrm{i} \xi_j x / N}, \ c_j \in \mathbb{C}, \ \xi_j \in B, \ \xi_k \neq \xi_j \text{ for } k \neq j \right\}$$

and its subspace with p equispaced frequencies

$$\Pi_B^p(A) := \left\{ g : A \to \mathbb{C} : g(x) = \sum_{j=0}^{p-1} c_j \mathrm{e}^{2\pi \mathrm{i} x \xi_j^B / N}, \ c_j \in \mathbb{C}, \ \xi_j^B := c^B + \beta_j w^B \right\}. \tag{2.2}$$

Let $C(A)$ denote the space of continuous functions on A and define the trigonometric interpolation operator

$$\mathcal{J}_p^{AB} : C(A) \to \Pi_B^p(A), \quad u \mapsto \mathcal{J}_p^{AB} u = \sum_{s=0}^{p-1} f_s \mathrm{e}^{2\pi \mathrm{i} x \xi_s^B / N}, \tag{2.3}$$

such that in the (shifted) Chebyshev nodes

$$x_r^A := c^A + \alpha_r w^A \tag{2.4}$$

the interpolation condition $\mathcal{J}_p^{AB} u(x_r^A) = u(x_r^A)$ for $r = 0, \dots, p-1$ holds true.

In order to show existence and uniqueness of this interpolation, we review polynomial interpolation in the complex plane. Let nodes $z_j \in \mathbb{C}$, $j = 0, \dots, p-1$, be distinct points and define the Lagrange polynomials $\widetilde{L}_k : \mathbb{C} \to \mathbb{C}$,

$$\widetilde{L}_k(z) = \prod_{\substack{j=0 \\ j \neq k}}^{p-1} \frac{z - z_j}{z_k - z_j}. \tag{2.5}$$

Of course, the unique polynomial in

$$\widetilde{\Pi}_{p-1}(\mathbb{C}) := \left\{ q : \mathbb{C} \to \mathbb{C} : q(z) = \sum_{j=0}^{p-1} c_j z^j : c_j \in \mathbb{C} \right\},$$

interpolating the data points $(z_j, f_j) \in \mathbb{C} \times \mathbb{C}$, $j = 0, \dots, p-1$, is given by $\sum_{j=0}^{p-1} f_j \widetilde{L}_j$. Hence, we have the following result.

Lemma 2.1. *Let $p \in \mathbb{N}$, $p \geq 2$, two boxes A and B and a function $u : A \to \mathbb{C}$, $u \in C(A)$, be given. Then, the interpolant* (2.3) *exists and is unique. Moreover, using the mappings*

$$z := z(x) = \mathrm{e}^{-2\pi \mathrm{i} x \frac{w^B}{(p-1)N}} \quad \text{and} \quad z_j := z(x_j^A)$$

to define the Lagrange functions

$$l_r^{AB}(x) = \widetilde{L}_r(z) = \prod_{\substack{j=0 \\ j \neq r}}^{p-1} \frac{z - z_j}{z_r - z_j}, \quad r = 0, \dots, p-1 \tag{2.6}$$

by means of the Lagrange polynomials (2.5)*, yields the representation*

$$\mathcal{J}_p^{AB} u(x) = \mathrm{e}^{2\pi \mathrm{i} \left(c^B + \frac{w^B}{2}\right) x/N} \sum_{r=0}^{p-1} u(x_r^A) \mathrm{e}^{-2\pi \mathrm{i} \left(c^B + \frac{w^B}{2}\right) x_r^A/N} l_r^{AB}(x). \tag{2.7}$$

Proof. Let $v : \mathbb{C} \to \mathbb{C}$ be continuous with $v(z) = v(z(x)) = u(x)$ for $x \in A$. The polynomial $q \in \widetilde{\Pi}_{p-1}(\mathbb{C})$, which interpolates the points $(z_r, v(z_r)) \in \mathbb{C} \times \mathbb{C}$, $r = 0, \dots, p-1$, is unique and given by

$$q(z) = \sum_{r=0}^{p-1} v(z_r) \widetilde{L}_r(z) = \sum_{r=0}^{p-1} u(x_r^A) l_r^{AB}(x).$$

The assertion follows, since the function

$$\mathrm{e}^{2\pi \mathrm{i} \left(c^B + \frac{w^B}{2}\right) \frac{x}{N}} \cdot q(z(x)) \cdot \mathrm{e}^{-2\pi \mathrm{i} \left(c^B + \frac{w^B}{2}\right) \frac{x_r^A}{N}}$$

lies in $\Pi_B^p(A)$ and interpolates the function u in the nodes x_r^A, $r = 0, \dots, p-1$. ∎

Remark 2.2. *In [15], the extremal points* $t_j^{\max} = \cos \frac{j}{p}\pi$, $j = 0, \dots, p$, *of the Chebyshev nodes were used in space and frequency domain. This yields a globally continuous approximant. In contrast, we use the Chebyshev nodes in space and equispaced nodes in frequency domain. While our subsequent error analysis is valid in both cases, the modification to equispaced nodes in frequency domain allows for an explicit, stable, and effective representation of the trigonometric interpolation operator in a Lagrange type basis.*

In contrast to [2, Thm. 3], where an interpolation by means of Lagrange polynomials with real nodes is used, we always interpolate with respect to the real spatial variable x *and by means of our Lagrange functions* l_r^{AB}, *which are Lagrange polynomials with complex nodes via the mapping in Lemma 2.1. In particular, interpolating a function from* $\Pi_B(A)$ *yields a function in its subspace* $\Pi_B^p(A)$.

For spatial dimension $d > 1$, a box is given as a Cartesian product $A = A^{(1)} \times \ldots \times A^{(d)}$, where $A^{(k)} = [a_k, b_k]$, $k = 0, \dots, d$, are one-dimensional boxes. We define the center and the width by

$$\boldsymbol{c}^A := \frac{1}{2}(a_1 + b_1, \dots, a_d + b_d)^\top, \quad w^A := \operatorname{diam}_\infty A := \max_{k=1,\dots,d}(b_k - a_k),$$

respectively. For boxes $A, B \subset \mathbb{R}^d$, we use tensor products of the spaces $\Pi_B(A)$ and $\Pi_B^p(A)$ and define the interpolation operator in a straightforward manner by

$$\mathcal{J}_p^{AB} = \bigotimes_{r=1}^{d} \mathcal{J}_p^{A^{(r)}B^{(r)}}.$$

2.1 Error analysis

In [15] a Taylor expansion of the complex exponential function has been used to motivate a restriction on the product of the widths of the boxes A and B. Subsequently, we present an error estimate for the interpolation $\mathcal{J}_p^{AB} g$ if $g \in \Pi_B(A)$ and A, B fulfil such an admissibility condition. The error estimate for the demodulated and thus smooth part relies on a standard argument for polynomial interpolation, modified here only for polynomials in a real variable and complex coefficients

$$\widetilde{\Pi}_{p-1}(A) := \left\{ q : \mathbb{R} \to \mathbb{C} : q(x) = \sum_{j=0}^{p-1} c_j x^j : c_j \in \mathbb{C} \right\}.$$

Of course, this polynomial interpolation can be expressed with respect to Lagrange polynomials, given for the Chebyshev nodes $\{x_j^A : j = 0, \dots, p-1\} \subset A \subset \mathbb{R}$ by

$$L_j^A(x) = \prod_{\substack{j=0 \\ j \neq k}}^{p-1} \frac{x - x_j^A}{x_k^A - x_j^A}, \tag{2.8}$$

where we drop the superscript if $A = [-1, 1]$.

Lemma 2.3. *Let* $p \in \mathbb{N}$, $A = [a, b]$, $a < b$, *and* $g : A \to \mathbb{C}$, $g \in C^p(A)$. *The polynomial interpolation* $\mathcal{I}_p^A : C(A) \to \widetilde{\Pi}_{p-1}(A)$,

$$\mathcal{I}_p^A g(x) = \sum_{j=0}^{p-1} g(x_j^A) L_j^A(x)$$

obeys

$$\left\|\mathcal{I}_p^A g - g\right\|_{C(A)} \leq \frac{(w^A)^p}{4^{(p-1)}p!}\|g^{(p)}\|_{C(A)}.$$

Proof. For real-valued $h : A \to \mathbb{R}$, $h \in C^p(A)$, we have $h(x) - \mathcal{I}_p^A h(x) = \frac{h^{(p)}(\xi(x))}{p!}\prod_{j=0}^{p-1}(x - x_j^A)$ for some $\xi(x) \in (a, b)$. Using

$$\max_{x\in A}\left|\prod_{j=0}^{p-1}(x - x_j^A)\right| = 2\left(\frac{w^A}{4}\right)^p \max_{x\in[-1,1]} T_p(x) \leq 2\left(\frac{w^A}{4}\right)^p$$

and linearity for the derivatives of $g = \operatorname{Re} g + \mathrm{i}\operatorname{Im} g$ yields the assertion. ∎

Theorem 2.4. *Let $p, N \in \mathbb{N}$, $p \geq 3$, two boxes $A, B \subset \mathbb{R}^d$ be admissible in the sense*

$$w^A w^B \leq N,$$

and $g \in \Pi_B(A)$, then we have the error estimate

$$\|g - \mathcal{J}_p^{AB} g\|_{C(A)} \leq ((C_p + 1)^d - 1)\|g\|_{C(A)}$$

and the operator norm bound

$$\|\mathcal{J}_p^{AB}\| = \sup_{\substack{g\in\Pi_B(A)\\ \|g\|_{C(A)}=1}} \|\mathcal{J}_p^{AB} g\|_{C(A)} \leq (C_p + 1)^d,$$

with the constant

$$C_p = \frac{2\pi^p}{4^{p-1}p! - \pi^p} \leq c_0 c_1^{-p}, \qquad c_0 = 216,\ c_1 = 6. \tag{2.9}$$

Proof. We start with the univariate case $d = 1$, $B = [k_{\min}, k_{\max}]$, $A = [x_{\min}, x_{\max}]$, and note that the trigonometric interpolation operator allows for shifts in the frequency domain, i.e.,

$$\mathcal{J}_p^{AB} \mathrm{e}^{2\pi\mathrm{i}kx} = \mathrm{e}^{2\pi\mathrm{i}k_0 x}\mathcal{J}_p^{A(B-k_0)}\mathrm{e}^{2\pi\mathrm{i}(k-k_0)x}.$$

Setting $k_0 = \frac{1}{2}(k_{\min} + k_{\max})$, the frequency-shifted function

$$\tilde{g}(x) = \sum_{k\in T} \hat{f}_k \mathrm{e}^{2\pi\mathrm{i}(k-k_0)x}$$

is slowly oscillating for $x \in A$ since A and B are admissible. Thus, the interpolation at the Chebyshev nodes by algebraic polynomials with complex coefficients yields

$$\|\mathcal{I}_p^A \tilde{g} - \tilde{g}\|_{C(A)} \leq \frac{(x_{\max} - x_{\min})^p}{4^{p-1}p!}\|\tilde{g}^{(p)}\|_{C(A)}.$$

Noting that the trigonometric and the algebraic interpolation coincide in the interpolation nodes yields $\mathcal{I}_p^X \tilde{g} = \mathcal{I}_p^A \mathcal{J}_p^{A(B-k_0)}\tilde{g}$ and hence

$$\left\|g - \mathcal{J}_p^{AB} g\right\|_{C(A)} = \left\|\mathrm{e}^{2\pi\mathrm{i}k_0 x}(\tilde{g} - \mathcal{J}_p^{A(B-k_0)}\tilde{g})\right\|_{C(A)}$$

$$
\begin{aligned}
&\leq \left\|\tilde{g} - \mathcal{I}_p^A \tilde{g}\right\|_{C(A)} + \left\|\mathcal{I}_p^A \tilde{g} - \mathcal{J}_p^{A(B-k_0)} \tilde{g}\right\|_{C(A)} \\
&= \left\|\tilde{g} - \mathcal{I}_p^A \tilde{g}\right\|_{C(A)} + \left\|\mathcal{I}_p^A \mathcal{J}_p^{A(B-k_0)} \tilde{g} - \mathcal{J}_p^{A(B-k_0)} \tilde{g}\right\|_{C(A)} \\
&\leq \frac{(x_{\max} - x_{\min})^p}{4^{p-1} p!} \left(\|\tilde{g}^{(p)}\|_{C(A)} + \left\| \left(\mathcal{J}_p^{A(B-k_0)} \tilde{g} \right)^{(p)} \right\|_{C(A)} \right).
\end{aligned}
$$

Since $\Pi_{B-k_0}(A)$ allows for a Bernstein inequality [17, p. 104] and due to the admissibility condition, we have

$$
\frac{(x_{\max} - x_{\min})^p}{4^{p-1} p!} \|\tilde{g}^{(p)}\|_{C(A)} \leq \frac{(x_{\max} - x_{\min})^p}{4^{p-1} p!} \left(\frac{\pi(k_{\max} - k_{\min})}{N} \right)^p \|\tilde{g}\|_{C(A)} \leq \frac{\pi^p}{4^{p-1} p!} \|\tilde{g}\|_{C(A)},
$$

which is true for $\|(\mathcal{J}_p^{A(B-k_0)} \tilde{g})^{(p)}\|_{C(A)}$ as well. Using the triangle inequality

$$
\left\|\mathcal{J}_p^{A(B-k_0)} \tilde{g}\right\|_{C(A)} \leq \left\|\mathcal{J}_p^{A(B-k_0)} \tilde{g} - \tilde{g}\right\|_{C(A)} + \|\tilde{g}\|_{C(A)}
$$

and bringing the error term to the left side yields the first assertion. The second claim simply follows by

$$
\|\mathcal{J}_p^{AB} g\|_{C(A)} \leq \|g - \mathcal{J}_p^{AB} g\|_{C(A)} + \|g\|_{C(A)}.
$$

Now, let $d > 1$ and $B = B^{(1)} \times \ldots \times B^{(d)}, A = A^{(1)} \times \ldots \times A^{(d)} \subset [0, N]^d$ be admissible. Since $\mathcal{J}_p^{AB} = \mathcal{J}_p^{A^{(1)}B^{(1)}} \otimes \ldots \otimes \mathcal{J}_p^{A^{(d)}B^{(d)}}$, the bound on the operator norm follows from the univariate case immediately. By slight abuse of notation we write $\mathcal{J}_p^{A^{(\nu)}B^{(\nu)}}$ also for the interpolation of a d-variate function in its ν-th variable and obtain the final error estimate

$$
\begin{aligned}
\left\|g - \mathcal{J}_p^{AB} g\right\|_{C(A)} &\leq \left\|g - \mathcal{J}_p^{A^{(1)}B^{(1)}} g\right\|_{C(A)} + \left\|\mathcal{J}_p^{A^{(1)}B^{(1)}} g - \mathcal{J}_p^{AB} g\right\|_{C(A)} \\
&\leq \sum_{\nu=1}^{d} \prod_{\mu=1}^{\nu-1} \left\|\mathcal{J}_p^{A^{(\mu)}B^{(\mu)}}\right\| \left\|g - \mathcal{J}_p^{A^{(\nu)}B^{(\nu)}} g\right\|_{C(A)} \\
&\leq C_p \|g\|_{C(A)} \sum_{\nu=1}^{d} (C_p + 1)^{\nu-1} \\
&= \left((C_p + 1)^d - 1 \right) \|g\|_{C(A)}.
\end{aligned}
$$

■

Of course, the given constants are just examples and one might trade a larger constant $c_0 = 3000$ for a stronger decrease $c_1 = 10$. Asymptotically, we have $\log C_p \leq -Cp \log p$ with some absolute constant $C > 0$.

2.2 Realisation

The local approximation by means of the interpolation operator needs to be realised using a basis for the ansatz space $\Pi_B^p(A)$. Subsequently, we discuss a variant of the original approach [15] which uses a monomial type basis and a new variant which relies on a Lagrange type basis. While both approaches take approximately the same amount of computation, the

latter is much more stable. In both cases, the univariate realisation generalises easily to the multivariate case since the tensor product structure of the interpolation operator just turns into a Kronecker product structure of the involved matrices.

Section 3 considers the butterfly scheme built upon the dyadic decomposition of the spatial domain X and the frequency domain T. For $A \subset X$ and $B \subset T$ admissible, this asks for the approximation $u^{AB} \in \Pi_B(A)$,

$$u^{AB} := \mathcal{J}_p^{AB} \sum_{S \in S_B} u^{PS}, \tag{2.10}$$

where

$$S_B = \left\{ \left[c^B - \frac{w^B}{2}, c^B \right], \left[c^B, c^B + \frac{w^B}{2} \right] \right\},$$

denotes the set of sons, for $d = 1$ at most two, of the set of frequencies

$$B = \left[c^B - \frac{w^B}{2}, c^B + \frac{w^B}{2} \right]$$

and the interpolation error is small in each of the spatial sets, for $d = 1$ again at most two,

$$A = \left[c^A - \frac{w^A}{2}, c^A + \frac{w^A}{2} \right],$$

which are subsets of their father

$$P = \left[c^P - \frac{w^P}{2}, c^P + \frac{w^P}{2} \right].$$

Subsequently, we rely on the admissibility condition $w^A w^B = N$ and on the dyadic decomposition which results in $w^P w^B = 2N$, see Figure 2.1 for an illustration of the sets.

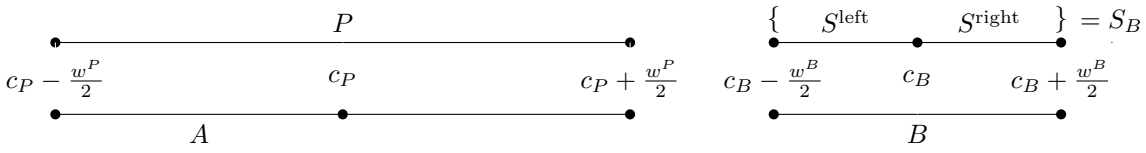

Figure 2.1: Illustration of the spatial set $A \subset P$ and frequency set $B \supset S_B$.

2.2.1 Monomial type basis

We closely follow the discussion in [15, Sect. 3.2] for solving the interpolation problem. The interpolant $\mathcal{J}_p^{AB} g$ for a function $g \in \Pi_B(A)$ is given by $g^{AB}(x) = \sum_{s=0}^{p-1} f_s^{AB} \mathrm{e}^{2\pi \mathrm{i} \xi_s^B x/N}(x)$ with the coefficient vector

$$\boldsymbol{f}^{AB} = \left(f_s^{AB}\right)_{s=0}^{p-1} = (\boldsymbol{M}^{AB})^{-1} \boldsymbol{g}^{AB}, \quad \boldsymbol{M}^{AB} = \left(\mathrm{e}^{2\pi \mathrm{i} \xi_s^B x_r^A/N}\right)_{r,s=0}^{p-1}, \; \boldsymbol{g}^{AB} = \left(g(x_r^A)\right)_{r=0}^{p-1}, \tag{2.11}$$

where we use the equally spaced nodes $\xi_s^B \in B$ and Chebyshev nodes $x_r^A \in A$, cf. (2.2) and (2.4). Using the two diagonal matrices

$$\boldsymbol{D}_1^{AB} = \operatorname{diag}\left(\mathrm{e}^{2\pi \mathrm{i}(c^A + \alpha_r w^A) c^B/N}\right)_{r=0}^{p-1}, \quad \boldsymbol{D}_2^{AB} = \operatorname{diag}\left(\mathrm{e}^{2\pi \mathrm{i} c^A \beta_s w^B/N}\right)_{s=0}^{p-1},$$

the matrix $\boldsymbol{M}^{AB} \in \mathbb{C}^{p\times p}$ can be factorised as

$$\boldsymbol{M}^{AB} = \boldsymbol{D}_1^{AB}\boldsymbol{G}\boldsymbol{D}_2^{AB}, \quad \boldsymbol{G} = \left(\mathrm{e}^{2\pi\mathrm{i}\alpha_r\beta_s}\right)_{r,s=0}^{p-1}, \tag{2.12}$$

where the matrix $\boldsymbol{G} \in \mathbb{C}^{p\times p}$ is independent of A and B. Applied to (2.10), this yields

$$\boldsymbol{f}^{AB} = \left(\boldsymbol{D}_2^{AB}\right)^{-1}\boldsymbol{G}^{-1}\left(\boldsymbol{D}_1^{AB}\right)^{-1}\boldsymbol{u}^{AB}, \quad \boldsymbol{u}^{AB} = \left(\sum_{S\in S_B} u^{PS}(x_r^A)\right)_{r=0}^{p-1}.$$

Given the coefficients $\boldsymbol{f}^{PS} = (f_s^{PS})_{s=0}^{p-1} \in \mathbb{C}^p$ in $u^{PS}(x) = \sum_{s=0}^{p-1} f_s^{PS}\mathrm{e}^{2\pi\mathrm{i}\xi_s^S x/N}$, we compute

$$\boldsymbol{u}^{AB} = \sum_{S\in S_B} \boldsymbol{N}^{AS}\boldsymbol{f}^{PS}, \quad \boldsymbol{N}^{AS} = \left(\mathrm{e}^{2\pi\mathrm{i}\xi_s^S x_r^A/N}\right)_{r,s=0}^{p-1}.$$

Again, using two diagonal matrices

$$\boldsymbol{E}_1^{AS} = \operatorname{diag}\left(\mathrm{e}^{2\pi\mathrm{i}(c^A+\alpha_r w^A)c^S/N}\right)_{r=0}^{p-1}, \quad \boldsymbol{E}_2^{AS} = \operatorname{diag}\left(\mathrm{e}^{2\pi\mathrm{i}c^A\beta_s w^S/N}\right)_{s=0}^{p-1},$$

we have an factorisation

$$\boldsymbol{N}^{AS} = \boldsymbol{E}_1^{AS}\boldsymbol{H}\boldsymbol{E}_2^{AS}, \quad \boldsymbol{H} = \left(\mathrm{e}^{\pi\mathrm{i}\alpha_r\beta_s}\right)_{r,s=0}^{p-1},$$

where the matrix $\boldsymbol{H} \in \mathbb{C}^{p\times p}$ is independent of A and B. Altogether, this yields

$$\boldsymbol{f}^{AB} = (\boldsymbol{D}_2^{AB})^{-1}\boldsymbol{G}^{-1}\sum_{S\in S_B}\boldsymbol{C}^{AS}\boldsymbol{H}\boldsymbol{E}_2^{AS}\boldsymbol{f}^{PS}, \quad \boldsymbol{C}^{AS} = \operatorname{diag}\left(\mathrm{e}^{\mp\pi\mathrm{i}\left(\frac{c^A}{w^A}+\alpha_r\right)/2}\right)_{r=0}^{p-1}, \tag{2.13}$$

where we have used

$$c^S - c^B = \begin{cases} -\frac{w^S}{2} & S \text{ is the left son of } B, \\ \frac{w^S}{2} & S \text{ is the right son of } B. \end{cases}$$

2.2.2 Lagrange type basis

Our new approach relies more directly on the definition (2.7) of the interpolant $\mathcal{J}_p^{AB}g$ for a function $g \in \Pi_B(A)$. Applied to (2.10) and in contrast to the variant above, the functions $u^{PS} \in \Pi_S(P)$, $S \in S_B$, are given by their function values $u^{PS}(x_r^P)$, $r = 0,\dots,p-1$, at the Chebyshev nodes in P and we compute the function values $u^{AB}(x_r^A)$, $r = 0,\dots,p-1$, at Chebyshev nodes in A. More detailed, we have

$$u^{AB}(x_r^A) = \sum_{S\in S_B} \mathrm{e}^{2\pi\mathrm{i}\left(c^S+\frac{w^S}{2}\right)x_r^A/N}\sum_{s=0}^{p-1} u^{PS}(x_s^P)\mathrm{e}^{-2\pi\mathrm{i}\left(c^S+\frac{w^S}{2}\right)x_s^P/N}\cdot l_s^{PS}(x_r^A). \tag{2.14}$$

The Lagrange polynomials are given via the mapping in Lemma 2.1 by

$$l_s^{PS}(x_r^A) = \prod_{\substack{j=0\\ j\neq s}}^{p-1}\frac{z(x_r^A)-z(x_j^P)}{z(x_s^P)-z(x_j^P)}.$$

Inserting $x_r^A = c^A + \alpha_r w^A$ and $x_j^P = c^P + \alpha_j w^P$ and using

$$c^A - c^P = \begin{cases} -\frac{w^A}{2} & A \text{ is the left son of } P, \\ \frac{w^A}{2} & A \text{ is the right son of } P, \end{cases}$$

yields

$$l_s^{PS}(x_r^A) = \begin{cases} \prod\limits_{\substack{j=0 \\ j\neq s}}^{p-1} \frac{\mathrm{e}^{-\pi\mathrm{i}\left(\alpha_r - \frac{1}{2}\right)/(p-1)} - \mathrm{e}^{-2\pi\mathrm{i}\frac{\alpha_j}{p-1}}}{\mathrm{e}^{-2\pi\mathrm{i}\frac{\alpha_s}{p-1}} - \mathrm{e}^{-2\pi\mathrm{i}\frac{\alpha_j}{p-1}}} & A \text{ is the left son of } P, \\ \prod\limits_{\substack{j=0 \\ j\neq s}}^{p-1} \frac{\mathrm{e}^{-\pi\mathrm{i}\left(\alpha_r + \frac{1}{2}\right)/(p-1)} - \mathrm{e}^{-2\pi\mathrm{i}\frac{\alpha_j}{p-1}}}{\mathrm{e}^{-2\pi\mathrm{i}\frac{\alpha_s}{p-1}} - \mathrm{e}^{-2\pi\mathrm{i}\frac{\alpha_j}{p-1}}} & A \text{ is the right son of } P. \end{cases} \tag{2.15}$$

With the vectors

$$\boldsymbol{u}^{PS} = \left(u^{PS}(x_r^P)\right)_{r=0}^{p-1}, \quad \boldsymbol{u}^{AB} = \left(u^{AB}(x_r^A)\right)_{r=0}^{p-1},$$

the diagonal matrices

$$\boldsymbol{R}^{AS} = \operatorname{diag}\left(\mathrm{e}^{2\pi\mathrm{i}\left(c^S + \frac{w^S}{2}\right)x_r^A/N}\right)_{r=0}^{p-1}, \quad \boldsymbol{S}^{PS} = \operatorname{diag}\left(\mathrm{e}^{-2\pi\mathrm{i}\left(c^S + \frac{w^S}{2}\right)x_s^P/N}\right)_{s=0}^{p-1},$$

and the Lagrange matrix, which depends only on the relation between A and P,

$$\boldsymbol{L}^A = \left(l_s^{PS}(x_r^A)\right)_{r,s=0}^{p-1}, \tag{2.16}$$

we finally obtain

$$\boldsymbol{u}^{AB} = \sum_{S \in S_B} \boldsymbol{R}^{AS} \boldsymbol{L}^A \boldsymbol{S}^{PS} \boldsymbol{u}^{PS}. \tag{2.17}$$

2.2.3 Computational complexity

The computation of the coefficients $\boldsymbol{f}^{AB}$ from the coefficients $\boldsymbol{f}^{PS}$ in (2.13) takes $\mathcal{O}(p^2)$ arithmetic operations, once the two matrices $\boldsymbol{G}^{-1}, \boldsymbol{H} \in \mathbb{C}^{p\times p}$ are set up. Similarly, the evaluation of $\boldsymbol{u}^{AB}$ from the function values $\boldsymbol{u}^{PS}$ in (2.17) takes $\mathcal{O}(p^2)$ arithmetic operations after precomputing the two Lagrange matrices $\boldsymbol{L}^A \in \mathbb{C}^{p\times p}$, $A \subset P$. Using the tensor product structure of the interpolation operator, the multivariate case clearly takes $\mathcal{O}(p^{d+1})$ arithmetic operations, see also [10] for an introduction to tensor and n-mode products.

Moreover, the matrices $\boldsymbol{G}^{-1}, \boldsymbol{H}, \boldsymbol{L}^A \in \mathbb{C}^{p\times p}$ are of Cauchy-Vandermonde type and thus allow for matrix vector multiplications in only $Cp\log^2 p$ floating point operations, cf. [6]. However note that p is hardly large enough in order that this consideration pays off in practice.

2.3 Stability

While implementing the original scheme [15], we found that the final accuracy of the butterfly sparse FFT is limited far above machine accuracy as shown in Section 4. Of course, the error of the local approximation and thus of the butterfly scheme decreases rapidly with increasing local expansion degree p - at least in precise arithmetic. On the other hand, we show subsequently that the condition number of the interpolation matrix $\boldsymbol{M}^{AB}$ strongly increases and thus rounding errors take over for larger p. Alternatively, we prove a weaker increase of the condition number of the Lagrange matrix $\boldsymbol{L}^A$ which seems to suffice for a stable butterfly sparse FFT. To compute the condition numbers, we need the following auxiliary estimates which are either standard or can be found e.g. as exercises in [13].

Lemma 2.5. *For $p \in \mathbb{N}$, $p \geq 3$, and $x \in \mathbb{R}$, $|x| \leq \frac{2\pi}{p-1}$, we have*

$$\cos \frac{2\pi}{p-1} \leq \cos x, \tag{2.18}$$

$$1 - \frac{x^2}{2} \leq \cos x, \tag{2.19}$$

$$\left(1 - \cos \frac{2\pi}{p-1}\right) \frac{(p-1)^2}{2\pi^2} \leq \frac{2(1-\cos x)}{x^2}, \tag{2.20}$$

$$\frac{16}{\pi^4} \leq \left(\frac{2(1-\cos x)}{x^2}\right)^{\frac{2\pi}{x}} \overset{x\to 0}{\longrightarrow} 1. \tag{2.21}$$

Proof. The first estimate follows since the cosine is decreasing in $[0, \frac{2\pi}{p-1}] \subset [0, \pi]$ and even. Integrating $\cos x \leq 1$ twice yields the second claim.

The relations $x \leq \tan x$ for $x \in [0, \frac{\pi}{2})$ and $\cos x \leq 0$, $\sin x \geq 0$, $x \geq 0$ for $x \in [\frac{\pi}{2}, \pi]$, yield $x \cos x - \sin x \leq 0$ and by integration

$$x \sin x - 2(1 - \cos x) \leq 0, \qquad x \in [0, \pi].$$

Dividing by $x^3/2$ this yields $f'(x) \leq 0$ for the even function $f(x) = \frac{2(1-\cos x)}{x^2}$ and thus $f(x) \geq f\left(\frac{2\pi}{p-1}\right)$, $|x| \leq \frac{2\pi}{p-1}$, which is the third assertion.

Considering $x \in [-\pi, 0)$, we have $0 < f(x) \leq 1$ and together with L'Hospitals rule

$$(f(x))^{\frac{2\pi}{x}} \geq 1, \ x \in [-\pi, 0), \quad \text{and} \quad \frac{2\pi}{x} \log f(x) \to 0, \ x \to 0.$$

Setting $g(x) = \frac{x}{2\pi} \log \frac{16}{\pi^4}$ and $h(x) = \log f(x)$ yields $g(0) = h(0)$, $g(\pi) = h(\pi)$, and

$$h''(x) = -\frac{1}{1-\cos x} + \frac{2}{x^2} \leq 0, \quad x \in [0, \pi].$$

Hence, the function h is concave and we obtain $h(x) \geq g(x)$. Since g is decreasing, this yields the assertion $\frac{2\pi}{x} h(x) \geq \log \frac{16}{\pi^4}$. ∎

Lemma 2.6. *For $p \in \mathbb{N}$, $p \geq 3$, the Chebyshev roots* (2.1) *and the coresponding Lagrange polynomials* (2.8) *obey*

$$\prod_{\substack{k=0 \\ k \neq n}}^{p-1} |t_k| = \frac{p}{2^{p-1}} \quad \text{if } p = 2n+1, \ n \in \mathbb{N}, \tag{2.22}$$

$$\max_{x \in [-1,1]} \sum_{s=0}^{p-1} (L_s(x))^2 \leq 2, \tag{2.23}$$

$$\max_{x \in [-3,3]} |L_s(x))| \leq \frac{34^{\frac{p}{2}}}{4p}. \tag{2.24}$$

Proof. Let $p = 2n+1$, $n \in \mathbb{N}$, then $t_n = 0$ and $L_n(0) = 1$. Moreover, we have $T_p'(0) = pU_{p-1}(0) = p$, where $U_{p-1}(\cos\theta) = \frac{\sin p\theta}{\sin \theta}$ denotes the Chebyshev polynomial of second kind. Via the representation

$$L_s(x) = \frac{T_p(x)}{(x - t_s) T_p'(t_s)} \tag{2.25}$$

and $T_p(x) = 2^{p-1}\prod_{j=0}^{p-1}(x - t_j)$ this yields for $x = 0$ the first assertion.

The Gauss-Chebyshev quadrature yields the discrete orthogonality

$$\sum_{s=0}^{p-1} T_k(t_s)T_l(t_s) = \begin{cases} 0 & \text{for } k \neq l, \\ p & \text{for } k = l = 0, \\ \frac{p}{2} & \text{for } k = l \neq 0, \end{cases}$$

and since $L_s(t_j) = \delta_{s,j}$ also the expansion of the Lagrange polynomials

$$L_s(x) = \frac{2}{p}\sum_{j=0}^{p-1}{}' T_j(t_s)T_j(x) := \frac{1}{p}T_0(t_s)T_0(x) + \frac{2}{p}\sum_{j=1}^{p-1} T_j(t_s)T_j(x),$$

where the prime indicates that the first summand is weighted by $\frac{1}{2}$. Hence, we have

$$\begin{aligned}\sum_{s=0}^{p-1}(L_s(x))^2 &= \sum_{s=0}^{p-1}\frac{4}{p^2}\left(\sum_{k=0}^{p-1}{}' T_k(t_s)T_k(x)\right)\left(\sum_{l=0}^{p-1}{}' T_l(t_s)T_l(x)\right) \\ &= \frac{4}{p^2}\sum_{k=0}^{p-1}{}'\sum_{l=0}^{p-1}{}' T_k(x)T_l(x)\sum_{s=0}^{p-1} T_k(t_s)T_l(t_s)\end{aligned}$$

and since $|T_k(x)| \leq 1$ for $x \in [-1, 1]$ the second claim by

$$\leq \frac{4}{p^2}\left(\frac{1}{4}p + (p-1)\frac{p}{2}\right) \leq 2.$$

Finally, we note that (2.23) implies $|L_s(x))| \leq \sqrt{2}$ for $|x| \leq 1$ and it remains to show the bound for $|x| \in [1, 3]$. Since L_s is a polynomial and has all its zeros inside $[-1, 1]$, it attains its extrema at $x = \pm 3$. Using once more (2.25), the explicit formula

$$T_k(x) = \frac{(x + \sqrt{x^2-1})^k + (x - \sqrt{x^2-1})^k}{2}, \quad |x| \geq 1,$$

the simple bound $(\pm 3 - t_s)^2 \geq 4$, and

$$(U_{p-1}(t_s))^2 = \frac{\sin^2\left(\frac{2s+1}{2}\pi\right)}{\sin^2\left(\frac{2s+1}{2p}\pi\right)} \geq \sin^2\left(\frac{2s+1}{2}\pi\right) = (-1)^{2s} = 1, \quad s = 0, \ldots, p-1,$$

we end at the last assertion. ∎

We are now prepared to prove the following bound on the stability of the local approximation scheme when the monomial type basis is used.

Theorem 2.7. *Let $p \in \mathbb{N}$, $p \geq 3$, and the local boxes be given as in Section 2.2. The (spectral) condition number of the interpolation matrix $\boldsymbol{M}^{AB}$ given in* (2.11) *fulfils*

$$\kappa(\boldsymbol{M}^{AB}) \geq \begin{cases} \sqrt{p}\left(\dfrac{p-1}{2\pi}\right)^{p-1} & p \geq 3, \quad (2.26) \\ \dfrac{1}{\sqrt{p}}\left(\dfrac{2(p-1)}{\pi}\right)^{p-1} & p \geq 3 \text{ and odd.} \quad (2.27) \end{cases}$$

Proof. We use the factorisations $\boldsymbol{M}^{AB} = \boldsymbol{D}_1^{AB}\boldsymbol{G}\boldsymbol{D}_2^{AB}$, see (2.12), and

$$\boldsymbol{G} = \boldsymbol{D}\boldsymbol{V}, \quad \boldsymbol{D} = \operatorname{diag}((\mathrm{e}^{\pi \mathrm{i}\alpha_r})_{r=0}^{p-1}), \quad \boldsymbol{V} = (z_r^s)_{r,s=0}^{p-1}, \quad z_r := \mathrm{e}^{-2\pi\mathrm{i}\frac{\alpha_r}{p-1}}.$$

Noting, that the norm of all the diagonal matrices and their inverse is equal to one, it suffices to analyse the Vandermonde matrix $\boldsymbol{V}$. We have

$$\|\boldsymbol{V}\|_2 = \sup_{\boldsymbol{x}\in\mathbb{C}^p\setminus\{0\}} \frac{\|\boldsymbol{V}\boldsymbol{x}\|_2}{\|\boldsymbol{x}\|_2} \geq \frac{\|\boldsymbol{V}\boldsymbol{e}_0\|_2}{\|\boldsymbol{e}_0\|_2} = \sqrt{p}.$$

for the zeroth unit vector $\boldsymbol{e}_0 = (1, 0, \ldots, 0)^\top \in \mathbb{C}^p$ and bound the norm $\|\boldsymbol{V}^{-1}\|_2$ by a similar technique.

Solving the linear system $\boldsymbol{V}\boldsymbol{f} = \boldsymbol{e}_0$ is equivalent to the polynomial interpolation problem

$$q : \mathbb{C} \to \mathbb{C}, \quad q(z) = \sum_{s=0}^{p-1} f_s z^s, \quad \text{such that} \quad q(z_r) = \delta_{r,0} \text{ for } r = 0, \ldots, p-1. \tag{2.28}$$

In terms of the Lagrange polynomials to the nodes $\{z_r\}_{r=0}^{p-1}$, its solution is given by

$$q(z) = \widetilde{L}_0(z) = \prod_{r=1}^{p-1} \frac{z - z_r}{z_0 - z_r} = \left(\prod_{r=1}^{p-1} \frac{1}{z_0 - z_r}\right) z^{p-1} + \ldots \quad .$$

and we consider the leading coefficient $f_{p-1} = \prod\limits_{r=1}^{p-1} \frac{1}{z_0 - z_r}$ in the monomial expansion (2.28). Applying Lemma 2.5, estimates (2.18) and (2.19), yields

$$\begin{aligned} |z_0 - z_r|^2 &= 2 - 2\cos\left(\frac{\pi}{p-1}\left(\cos\frac{\pi}{2p} - \cos\frac{2r+1}{2p}\pi\right)\right) \\ &\leq 2 - 2\cos\frac{2\pi}{p-1} \leq 2 - 2\left(1 - \frac{4\pi^2}{2(p-1)^2}\right) = \left(\frac{2\pi}{p-1}\right)^2. \end{aligned}$$

Hence, we obtain

$$\|\boldsymbol{V}^{-1}\|_2 \geq \|\boldsymbol{V}^{-1}\boldsymbol{e}_0\|_2 \geq |f_{p-1}| = \prod_{r=1}^{p-1} \frac{1}{|z_0 - z_r|} \geq \left(\frac{p-1}{2\pi}\right)^{p-1}$$

and thus the assertion (2.26).

For $p = 2n+1$, $n \in \mathbb{N}$, we consider the linear system $\boldsymbol{V}\boldsymbol{f} = \boldsymbol{e}_n$ with the n-th unit vector, which is equivalent to the interpolation problem

$$q : \mathbb{C} \to \mathbb{C}, \quad q(z) = \sum_{s=0}^{p-1} f_s z^s, \quad \text{such that} \quad q(z_r) = \delta_{n,r} \text{ for } r = 0, \ldots, p-1.$$

Noting $z_n = 1$ and analogously to the above consideration, we have

$$q(z) = \widetilde{L}_n(z) = \prod_{\substack{k=0 \\ k\neq n}}^{p-1} \frac{z - z_k}{1 - z_k} = f_{p-1}z^{p-1} + \ldots \quad , \; f_{p-1} = \prod_{\substack{k=0 \\ k\neq n}}^{p-1} \frac{1}{1 - z_k}.$$

Using Lemma 2.5 (2.19) yields

$$|1 - z_k|^2 = 2 - 2\cos\frac{\pi}{p-1}t_k \leq \frac{\pi^2}{(p-1)^2}t_k^2$$

and together with Lemma 2.6 (2.22) the assertion (2.27) since

$$\|\boldsymbol{V}^{-1}\|_2 \geq |f_{p-1}| \geq \left(\frac{p-1}{\pi}\right)^{p-1} \prod_{\substack{k=0 \\ k\neq n}}^{p-1} |t_k|^{-1} = \frac{2^{p-1}}{p}\left(\frac{p-1}{\pi}\right)^{p-1}.$$

■

The condition number of the matrix $\boldsymbol{N}^{AS}$ in Section 2.2.1 can be analysed in the same way to yield $\kappa(\boldsymbol{N}^{AS}) \approx 2^{p-1}\kappa(\boldsymbol{M}^{AB})$. In contrast to the lower bound on the conditioning of the original method, we obtain an upper bound for the local approximation scheme when the Lagrange type basis, cf. Section 2.2.2, is used.

Theorem 2.8. *Under the assumptions of Theorem 2.7, the (spectral) condition number of the Lagrange interpolation matrix* $\boldsymbol{L}^A$ *given in* (2.16) *fulfils*

$$\kappa\left(\boldsymbol{L}^A\right) \leq K_p \frac{\sqrt{2p \cdot 34^p}}{4} \leq \frac{\sqrt{2p}}{4} \cdot 6^{p+1}, \quad K_p = \left(\frac{2\pi^2}{\left(1 - \cos\frac{2\pi}{p-1}\right)(p-1)^2}\right)^{p-1},$$

and $\lim_{p\to\infty} K_p = 1$.

Proof. The Lagrange functions (2.15) are independent of the box A, up to its relation to the father box P. Setting $x_r = \alpha_r \mp \frac{1}{2}$ in (2.15) yields

$$|l_s^{PS}(x_r^A)|^2 = \prod_{\substack{j=0 \\ j\neq s}}^{p-1} \frac{1 - \cos\left(\frac{2\pi}{p-1}(\alpha_j - \frac{x_r}{2})\right)}{1 - \cos\left(\frac{2\pi}{p-1}(\alpha_j - \alpha_s)\right)}.$$

Since $x_r \in [-1,1]$ and thus $\alpha_j - \frac{x_r}{2} \in [-1,1]$, we apply Lemma 2.5, estimates (2.20) and (2.19), to obtain the relations

$$\begin{aligned} &\leq \prod_{\substack{j=0 \\ j\neq s}}^{p-1} \frac{4\pi^2}{2\left(1 - \cos\frac{2\pi}{p-1}\right)(p-1)^2} \frac{(\alpha_j - \frac{x_r}{2})^2}{(\alpha_j - \alpha_s)^2} \\ &= K_p \prod_{\substack{j=0 \\ j\neq s}}^{p-1} \left(\frac{x_r - t_j}{t_s - t_j}\right)^2 = K_p \cdot \left(L_s(x_r)\right)^2. \end{aligned}$$

Due to inequality (2.23) in Lemma 2.6, this yields

$$\|\boldsymbol{L}^A\|_{\mathrm{F}}^2 = \sum_{r=0}^{p-1}\sum_{s=0}^{p-1} |l_s^{PS}(x_r^A)|^2 \leq K_p \sum_{r=0}^{p-1} \max_{x\in[-1,1]} \sum_{s=0}^{p-1} (L_s(x))^2 \leq 2pK_p. \tag{2.29}$$

In view of the related polynomial interpolation problem on the complex unit circle and by changing the basis of the Lagrange polynomials l_s^{PS} to l_s^{AS}, the entries of the inverse Lagrange matrix can be written as

$$\left(\left(\boldsymbol{L}^A\right)^{-1}\right)_{r,s} = l_s^{AS}(x_r^P) = \begin{cases} \prod\limits_{\substack{j=0\\ j\neq s}}^{p-1} \frac{\mathrm{e}^{-\pi\mathrm{i}\left(2\alpha_r+\frac{1}{2}\right)/(p-1)} - \mathrm{e}^{-\pi\mathrm{i}\frac{\alpha_j}{p-1}}}{\mathrm{e}^{-\pi\mathrm{i}\frac{\alpha_s}{p-1}} - \mathrm{e}^{-\pi\mathrm{i}\frac{\alpha_j}{p-1}}} & A \text{ is the left son of } P, \\ \prod\limits_{\substack{j=0\\ j\neq s}}^{p-1} \frac{\mathrm{e}^{-\pi\mathrm{i}\left(2\alpha_r-\frac{1}{2}\right)/(p-1)} - \mathrm{e}^{-\pi\mathrm{i}\frac{\alpha_j}{p-1}}}{\mathrm{e}^{-\pi\mathrm{i}\frac{\alpha_s}{p-1}} - \mathrm{e}^{-\pi\mathrm{i}\frac{\alpha_j}{p-1}}} & A \text{ is the right son of } P. \end{cases}$$

Analogously to the first part of the proof, we set $x_r = 2\alpha_r \pm \frac{1}{2} \subset \left[-\frac{3}{2}, \frac{3}{2}\right]$ and use $\alpha_j - x_r \in [-2, 2]$ to apply Lemma 2.5, estimates (2.20) and (2.19). Together with $2x_r \in [-3, 3]$, inequality (2.24) in Lemma 2.6 yields

$$|l_s^{AS}(x_r^P)|^2 = \prod_{\substack{j=0\\ j\neq s}}^{p-1} \frac{1-\cos\left(\frac{\pi}{p-1}(\alpha_j - x_r)\right)}{1-\cos\left(\frac{\pi}{p-1}(\alpha_j - \alpha_s)\right)} \leq K_p \cdot (L_s(2x_r))^2 \leq \frac{34^p K_p}{16p^2}.$$

Combining (2.29) and the slightly simpler estimate

$$\| \left(\boldsymbol{L}^A\right)^{-1} \|_{\mathrm{F}}^2 = \sum_{r=0}^{p-1}\sum_{s=0}^{p-1} |l_s^{AS}(x_r^P)|^2 \leq \frac{34^p K_p}{16},$$

the assertion follows by bounding the spectral norm by the Frobenius norm. Setting $x = \frac{2\pi}{p-1}$ in Lemma 2.5 (2.21) finally yields $\lim_{p\to\infty} K_p = 1$ and $K_p\sqrt{34} \leq 6^2$. ∎

3 Butterfly scheme

As pointed out in the introduction, we aim to compute

$$u_j = u(\boldsymbol{x}_j) = \sum_{k=1}^{M_2} \hat{f}_k \mathrm{e}^{2\pi\mathrm{i}\boldsymbol{\xi}_k \boldsymbol{x}_j}, \quad j = 1, \ldots, M_1, \tag{3.1}$$

for a space dimension $d \in \mathbb{N}$, a nonharmonic bandwidth $N = 2^L$, $L \in \mathbb{N}$, a set of frequencies $\tilde{T} = \{\boldsymbol{\xi}_k \in [0, N]^d : k = 1, \ldots, M_2\}$, a set of Fourier coefficients $\hat{f}_k \in \mathbb{C}$, $k = 1, \ldots, M_2$, and a set of evaluation nodes $\tilde{X} = \{\boldsymbol{x}_j \in [0, N]^d : j = 1, \ldots, M_1\}$. For $d = 1$ and no restrictions on the sampling sets $\tilde{T}$ and $\tilde{X}$, the following considerations just give a slightly more expensive variant of the FFT for nonequispaced data in space and frequency domain [5, 8], but we include this case for notational convenience. In case $d \geq 2$, $M_1 = M_2 = N^{d-1}$, and well distributed sampling sets on smooth $d-1$ dimensional manifolds, the following dyadic decompositions of the sampling sets remain sparse. The butterfly graph, which represents the admissible pairs where computations are performed, remains sparse as well and a favourable complexity can be achieved.

In the one dimensional case, we consider $T := X := [0, N]$ and the dyadic decomposition

$$X_{l,m} \quad := \left[N/2^l m, N/2^l(m+1)\right) \qquad \text{for } m = 0, \ldots, 2^l - 1,$$

$$T_{L-l,n} := \big[N/2^{L-l}n, N/2^{L-l}(n+1)\big) \qquad \text{for } n = 0, \dots, 2^{L-l} - 1,$$

for $l = 0, \dots, L$, where the level in the butterfly scheme and locations are denoted by l and m, n, respectively. Moreover note that we always include the point N in the rightmost sets $X_{l,2^l-1}$ and $T_{l,2^l-1}$, $l = 0, \dots, L$. The decomposition of the interval $X = [0, N]$ is illustrated in Figure 3.1, all in the sense of Theorem 2.4 admissible pairs $(X_{l,m}, T_{L-l,n})$ are shown in Figure 3.2.

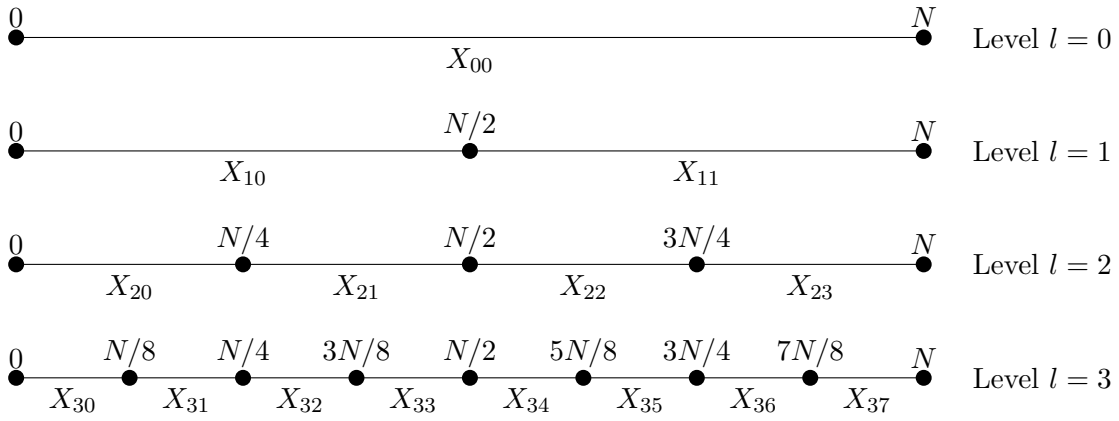

Figure 3.1: Dyadic decomposition of X.

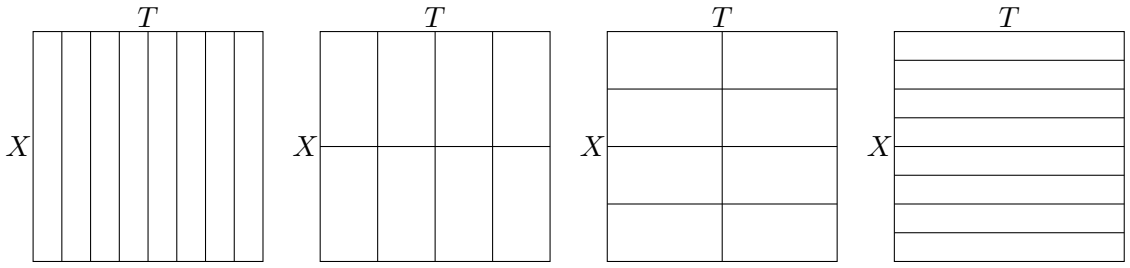

(a) Level $l = 0$. (b) Level $l = 1$. (c) Level $l = 2$. (d) Level $l = 3$.

Figure 3.2: Admissible pairs of $X = T = [0, 8]$.

If we represent all intervals of the two dyadic decomposition by a node in a graph and have edges for inclusions, we obtain two binary trees. Furthermore, all admissible pairs $(X_{l,m}, T_{L-l,n})$ are nodes in the butterfly graph, they are given as combinations of nodes in the l-th level of the X-tree and the $(L-l)$-th level in the T-tree. An edge is set if and only if the nodes in the X-tree and in the T-tree are connected, see Figure 3.3.

For spatial dimension $d \geq 2$, we have $T := X := [0, N]^d$ and decompose dyadically for levels $l = 0, \dots, L$ into the boxes

$$X_{l,\boldsymbol{m}} := X_{l,m_1} \times \ldots \times X_{l,m_d}, \quad T_{L-l,\boldsymbol{n}} := T_{L-l,n_1} \times \ldots \times T_{L-l,n_d},$$

with the location parameters $\boldsymbol{m} := (m_1, \dots, m_d)$, $0 \leq m_1, \dots, m_d \leq 2^l - 1$, and $\boldsymbol{n} := (n_1, \dots, n_d)$, $0 \leq n_1, \dots, n_d \leq 2^{L-l} - 1$.

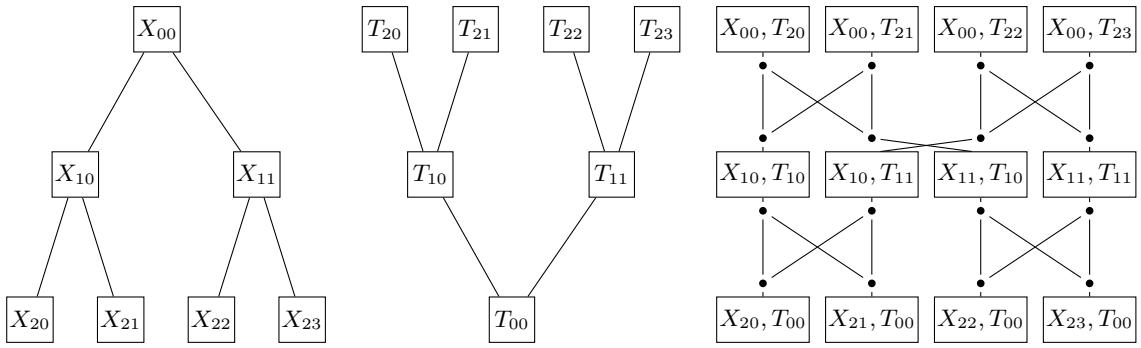

(a) X-tree. (b) T-tree. (c) Butterfly graph.

Figure 3.3: Trees and butterfly graph for $N = 4$.

The butterfly scheme in Algorithm 1 now traverses the butterfly graph top down. Starting from level $l = 0$ and local sums over frequencies, we define in each level approximations from its two predecessors. Level by level, they include more frequencies and are valid in smaller spatial boxes. The final approximation is a function piecewise defined in the smallest X-boxes.

3.1 Error analysis

In contrast to other analysis-based fast algorithms, the butterfly scheme uses a sequence of approximations and the local expansion degree depends not only on the target accuracy $\varepsilon > 0$ but also mildly on the nonharmonic bandwidth N. This behaviour is illustrated also numerically in Section 4.2.

Theorem 3.1. *Let $L \in \mathbb{N}$, $N = 2^L$, $T, X \subset [0, N]^d$, and $p \in \mathbb{N}$, $p \geq 3$, then the approximation* (3.4) *to the function* (3.1) *obeys the error estimate*

$$\|u - \tilde{u}\|_{C(X)} \leq \Big((1 + C_p)^{d(L+1)} - 1\Big) \|\hat{\boldsymbol{f}}\|_1.$$

Proof. Define for all levels $l = 0, \dots, L$ and the spatial indices $\boldsymbol{m} \in \mathbb{N}_0^d$, $\|\boldsymbol{m}\|_\infty < 2^l$, the error term

$$E_{l,\boldsymbol{m}} := \sum_{\boldsymbol{n} \in \mathbb{N}_0^d; \|\boldsymbol{n}\|_\infty < 2^{L-l}} \|u^{T_{L-l,\boldsymbol{n}}} - u^{X_{l,\boldsymbol{m}} T_{L-l,\boldsymbol{n}}}\|_{C(X_{l,\boldsymbol{m}})},$$

which by definition fulfils $\|u - \tilde{u}\|_{C(X)} = \max_{\boldsymbol{m} \in \mathbb{N}_0^d, \|\boldsymbol{m}\|_\infty < 2^l} E_{L,\boldsymbol{m}}$. Using Theorem 2.4 and the triangle inequality, this quantity can be bounded for the zeroth level by

$$\begin{aligned} E_{0,\mathbf{0}} &= \sum_{\boldsymbol{n} \in \mathbb{N}_0^d; \|\boldsymbol{n}\|_\infty < 2^L} \|u^{T_{L,\boldsymbol{n}}} - \mathcal{J}_p^{X_{0,\mathbf{0}} T_{L,\boldsymbol{n}}} u^{T_{L,\boldsymbol{n}}}\|_{C(X_{0,\mathbf{0}})} \\ &\leq \Big((C_p + 1)^d - 1\Big) \sum_{\boldsymbol{n} \in \mathbb{N}_0^d; \|\boldsymbol{n}\|_\infty < 2^L} \|u^{T_{L,\boldsymbol{n}}}\|_{C(X_{0,\mathbf{0}})} \leq ((C_p + 1)^d - 1) \|\hat{\boldsymbol{f}}\|_1. \end{aligned}$$

For $l > 0$, adding and subtracting the term $\mathcal{J}_p^{X_{l,\boldsymbol{m}} T_{L-l,\boldsymbol{n}}} u^{T_{L-l,\boldsymbol{n}}}$ yields

$$E_{l,\boldsymbol{m}} = \sum_{\substack{\boldsymbol{n} \in \mathbb{N}_0^d \\ \|\boldsymbol{n}\|_\infty < 2^{L-l}}} \|u^{T_{L-l,\boldsymbol{n}}} - \mathcal{J}_p^{X_{l,\boldsymbol{m}} T_{L-l,\boldsymbol{n}}} u^{T_{L-l,\boldsymbol{n}}} + \mathcal{J}_p^{X_{l,\boldsymbol{m}} T_{L-l,\boldsymbol{n}}} u^{T_{L-l,\boldsymbol{n}}} - u^{X_{l,\boldsymbol{m}} T_{L-l,\boldsymbol{n}}}\|_{C(X_{l,\boldsymbol{m}})}.$$

Algorithm 1 Butterfly scheme.

Input: $d, L, M_1, M_2, p \in \mathbb{N}$, $p \geq 3$, $N = 2^L$,
$\hat{f}_k \in \mathbb{C}$, $\boldsymbol{\xi}_k \in [0, N]^d$, $k = 1, \ldots, M_2$,
$\boldsymbol{x}_j \in [0, N]^d$, $j = 1, \ldots, M_1$.

for $n_1, \ldots, n_d = 0, \ldots, 2^L$ ***do***

$$u^{T_{L,\boldsymbol{n}}}(\boldsymbol{x}) := \sum_{\boldsymbol{\xi}_k \in T_{L,\boldsymbol{n}} \cap \widetilde{T}} \hat{f}_k \mathrm{e}^{2\pi \mathrm{i} \boldsymbol{\xi}_k \cdot \boldsymbol{x}/N} \tag{3.2}$$
$$u^{X_{0,\mathbf{0}} T_{L,\boldsymbol{n}}} := \mathcal{J}_p^{X_{0,\mathbf{0}} T_{L,\boldsymbol{n}}} u^{T_{L,\boldsymbol{n}}}$$

end for

for $l = 1, \ldots, L$ ***do***
for $m_1, \ldots, m_d = 0, \ldots, 2^l$ and $n_1, \ldots, n_d = 0, \ldots, 2^{L-l}$ ***do***

$$u^{X_{l,\boldsymbol{m}} T_{L-l,\boldsymbol{n}}} := \mathcal{J}_p^{X_{l,\boldsymbol{m}} T_{L-l,\boldsymbol{n}}} \sum_{\boldsymbol{k} \in \{0,1\}^d} u^{X_{l-1,\lfloor \boldsymbol{m}/2 \rfloor} T_{L-l+1,2\boldsymbol{n}+\boldsymbol{k}}} \tag{3.3}$$

end for

end for

for $j = 1, \ldots, M_1$ ***do***

$$\boldsymbol{m} := \lfloor \boldsymbol{x}_j \rfloor$$
$$\tilde{u}(\boldsymbol{x}_j) := u^{X_{L,\boldsymbol{m}} T_{0,\mathbf{0}}}(\boldsymbol{x}_j) \tag{3.4}$$

end for

Output: Approximate function values $\tilde{u}(\boldsymbol{x}_j)$, $j = 1, \ldots, M_1$.

Using the triangle inequality, the first norm can be bounded as for the zeroth level, and we proceed by applying equation (3.3), factoring out the interpolation operator, using the dyadic decomposition $T_{L-l,\boldsymbol{n}} = \cup_{\boldsymbol{k} \in \{0,1\}^d} T_{L-l+1,2\boldsymbol{n}+\boldsymbol{k}}$, and the relation $X_{l,\boldsymbol{m}} \subset X_{l-1,\lfloor \boldsymbol{m}/2 \rfloor}$ to obtain

$$\begin{aligned}
&\sum_{\substack{\boldsymbol{n} \in \mathbb{N}_0^d \\ \|\boldsymbol{n}\|_\infty < 2^{L-l}}} \|\mathcal{J}_p^{X_{l,\boldsymbol{m}} T_{L-l,\boldsymbol{n}}} u^{T_{L-l,\boldsymbol{n}}} - u^{X_{l,\boldsymbol{m}} T_{L-l,\boldsymbol{n}}}\|_{C(X_{l,\boldsymbol{m}})} \\
&\leq \sum_{\substack{\boldsymbol{n} \in \mathbb{N}_0^d \\ \|\boldsymbol{n}\|_\infty < 2^{L-l}}} \left\|\mathcal{J}_p^{X_{l,\boldsymbol{m}} T_{L-l,\boldsymbol{n}}}\right\| \sum_{\boldsymbol{k} \in \{0,1\}^d} \left\|u^{T_{L-l+1,2\boldsymbol{n}+\boldsymbol{k}}} - u^{X_{l-1,\lfloor \boldsymbol{m}/2 \rfloor} T_{L-l+1,2\boldsymbol{n}+\boldsymbol{k}}}\right\|_{C(X_{l-1,\lfloor \frac{\boldsymbol{m}}{2} \rfloor})} \\
&\leq (C_p + 1)^d E_{l-1,\lfloor \frac{\boldsymbol{m}}{2} \rfloor}.
\end{aligned}$$

Hence, we inductively find for $\boldsymbol{m} \in \mathbb{N}_0^d$, $\|\boldsymbol{m}\|_\infty < 2^L$, the assertion

$$E_{L,\boldsymbol{m}} \leq ((C_p + 1)^d - 1)\|\hat{\boldsymbol{f}}\|_1 + (C_p + 1)^d E_{L-1,\lfloor \frac{\boldsymbol{m}}{2} \rfloor} \leq ((C_p + 1)^{d(L+1)} - 1)\|\hat{\boldsymbol{f}}\|_1.$$

■

Corollary 3.2. *Under the assumptions of Theorem 3.1, let for given $\varepsilon \in (0,1]$ the expansion degree $p \in \mathbb{N}$, $p \geq 3$, fulfil*

$$p \geq \frac{1}{\log c_1} \left(|\log \varepsilon| + \log(L+1) + \log(2c_0 d) \right),$$

then

$$\|u - \tilde{u}\|_{C(X)} \leq \varepsilon \|\hat{\boldsymbol{f}}\|_1$$

Proof. Clearly, we have $(1+C_p)^{d(L+1)} - 1 \leq \varepsilon$ if and only if $d(L+1)\log(1+C_p) \leq \log(1+\varepsilon)$. Using simple bounds on the logarithm

$$\log(1+C_p) \leq C_p, \qquad \log(1+\varepsilon) \geq \frac{\varepsilon}{2},$$

yields the condition $2d(L+1)C_p = 2d(L+1)c_0 c_1^{-p} \leq \varepsilon$ for which the above assumption is sufficient. ∎

3.2 Computational complexity

Again, we start with the univariate case $d = 1$. For the level $l = 0$, the local sums $u^{T_{L,n}}$ in (3.2) are evaluated at Chebychev nodes x_r^X, $r = 0, \ldots, p-1$, and this takes $\mathcal{O}(pM_2)$ floating point operations. For each level $l = 0, \ldots, L$, we have to apply the interpolation operator $N = 2^L$ times and a single application takes $\mathcal{O}(p^2)$ floating point operations, cf. Section 2.2.3. Finally, we evaluate the function $\tilde{u}(x_j)$ at all sampling nodes, which takes $\mathcal{O}(pM_1)$ floating point operations for the original approach [15] and the approach in Section 2.2.2 with precomputation of the Lagrange functions at the evaluation nodes. Without such precomputations, a straightforward evaluation of the Lagrange functions leads to $\mathcal{O}(p^2 M_1)$ floating point operations for this step. Assuming $M_1, M_2 = \mathcal{O}(N)$ and a target accuracy $\varepsilon > 0$, this sums up to the total computational costs $\mathcal{O}(N \log N(|\log \varepsilon| + \log\log N)^2)$.

Generalising to $d \geq 2$, we assume that the sets $\tilde{T}, \tilde{X} \subset [0,N]^d$ and their dyadic subdivisions are sparse in the sense

$$|\{\boldsymbol{m} \in \mathbb{N}_0^d : m_1, \ldots, m_d \leq 2^l - 1,\ \tilde{X} \cap X_{l,\boldsymbol{m}} \neq \emptyset\}| \leq C 2^{(d-1)l},$$
$$|\{\boldsymbol{n} \in \mathbb{N}_0^d : n_1, \ldots, n_d \leq 2^{L-l} - 1,\ \tilde{T} \cap T_{L-l,\boldsymbol{m}} \neq \emptyset\}| \leq C 2^{(d-1)(L-l)}$$

for some absolute constant $C \in \mathbb{R}$. In particular, $M_1 = |\tilde{X}|$ and $M_2 = |\tilde{T}|$ fulfil $M_1, M_2 = \mathcal{O}(N^{d-1})$ and the above condition is satisfied if the sets lie on some smooth $(d-1)$-dimensional manifold in $[0,N]^d$, see also Figure [15, Fig. 5]. Under this sparsity assumption, the number of admissible pairs on which we need to compute is $\mathcal{O}(N^{d-1})$ in each level of the butterfly scheme and a single application of the interpolation operator takes $\mathcal{O}(p^{d+1})$ floating point operations. Finally, the evaluation of the function $\tilde{u}(\boldsymbol{x}_j)$ at all sampling nodes takes $\mathcal{O}(p^d M_1)$ floating point operations in all approaches, in case of on-the-fly evaluation of the Lagrange functions in tensor product form the costs are amortized. In total this sums up to computational costs $\mathcal{O}(N \log N(|\log \varepsilon| + \log\log N)^{d+1})$. The exponent $d+1$ of the last term can be decreased to d by using $\log C_p \leq -Cp \log p$ and the techniques in [6]. A similar improvement might be possible by reducing the p^d dimensional ansatz to one which lives on the $d-1$ dimensional manifold.

4 Numerical experiments

The implementation of the butterfly sparse FFT is realised in MATLAB 7.10.0 (R2010a) for the dimensions $d = 1, 2, 3, 4$. We use one node of a Dell PowerEdge R900, 96GByte, 2.4GHz Intel Xeon 7450, CentOS5.5, for all numerical experiments.

4.1 Local accuracy and stability

The first two experiments are dedicated to the approximation in one pair of admissible boxes. Let the nonharmonic bandwidth $N = 2^L$, $L = 10, 14$, the level $l = 5$, and the boxes $A = [0, 2^l]$, $B = [0, 2^{L-l}]$ be given. Draw nodes $x_j \in A$, $j = 1, \ldots, M_1$, $M_1 = N$, and $\xi_k \in B$, $k = 1, \ldots, M_2$, $M_2 = N$, at random from the uniform distribution and define the Fourier matrix

$$\boldsymbol{F} := \left(\mathrm{e}^{2\pi\mathrm{i}\xi_k \cdot x_j/N}\right)_{j=1,k=1}^{M_1,M_2}.$$

This matrix is approximately of low rank and we consider the expansions from Sections 2.2.1 and 2.2.2,

$$\tilde{\boldsymbol{F}} := \boldsymbol{F}^A (\boldsymbol{M}^{AB})^{-1} \boldsymbol{F}^B \quad \text{or} \quad \tilde{\boldsymbol{F}} := \tilde{\boldsymbol{L}}^A \boldsymbol{F}^B$$

with the auxiliary matrices

$$\boldsymbol{F}^A := \left(\mathrm{e}^{2\pi\mathrm{i}\xi_s^B x_j/N}\right)_{j=1,s=0}^{M_1,p-1}, \quad \boldsymbol{F}^B := \left(\mathrm{e}^{2\pi\mathrm{i}\xi_k x_r^A/N}\right)_{r=0,k=1}^{p-1,M_2},$$
$$\tilde{\boldsymbol{L}}^A := \left(\mathrm{e}^{2\pi\mathrm{i}\left(c^B + \frac{w^B}{2}\right)x_j/N} l_r^{AB}(x_j) \mathrm{e}^{-2\pi\mathrm{i}\left(c^B + \frac{w^B}{2}\right)x_r^A/N}\right)_{j=1,r=0}^{M_1,p-1},$$

respectively. In both cases, Theorem 2.4 assures

$$\varepsilon_1 := \max_{\substack{\hat{\boldsymbol{f}} \in \mathbb{C}^{M_2} \\ \|\hat{\boldsymbol{f}}\|_1 = 1}} \left\| \boldsymbol{F}\hat{\boldsymbol{f}} - \tilde{\boldsymbol{F}}\hat{\boldsymbol{f}} \right\|_\infty = \max_{\substack{j=1,\ldots,M_1 \\ k=1,\ldots,M_2}} \left| \boldsymbol{F}_{j,k} - \tilde{\boldsymbol{F}}_{j,k} \right| \leq c_0 c_1^{-p}.$$

We compare the quantity ε_1 for both realisations and for the original approach [15] in Figure 4.1. The original scheme differs from the variant in Section 2.2.1 in the choice of interpolation nodes in $x_r^A \in A$, where we use zeros of Chebychev polynomials instead of extrema, and in the choice of the 'equivalent sources' $\xi_s^B \in B$, where we use equidistant points instead of Chebyshev extrema. In all three cases, the error decays exponentially with increasing expansion degree p as predicted by Theorem 2.4. However note that both monomial type approaches achieve only an accuracy $\varepsilon_1 \approx 10^{-8}$ and suffer from severe instabilities for values $p \geq 9$ which is well predicted by the quantity $\boldsymbol{M}^{AB}\mu$, where $\mu \approx 2 \cdot 10^{-16}$ denotes the machine precision.

The second experiment analyses the stability of the monomial and the Lagrange type approaches as theoretically discussed in Section 2.3. Figure 4.2 shows the growth of the condition numbers of the matrices $\boldsymbol{M}^{AB}$, $\boldsymbol{L}^A \in \mathbb{C}^{p \times p}$, and lower and upper bounds, cf. Theorems 2.7 and 2.8.

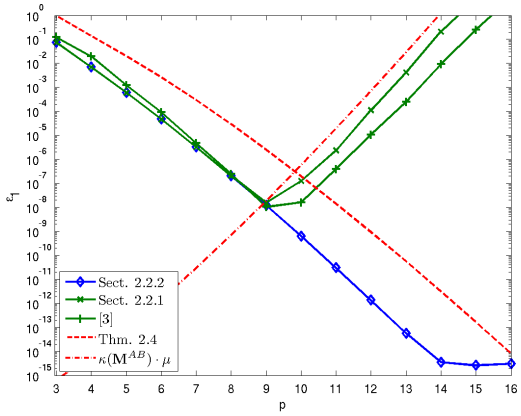

(a) $N = 2^{10}$ and $l = 5$.

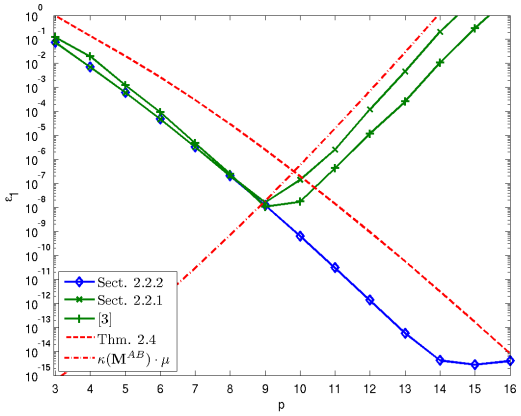

(b) $N = 2^{14}$ and $l = 5$.

Figure 4.1: Relative error ε_1 with respect to the local expansion degree p for the realisation via Lagrange functions, cf. Section 2.2.2, and monomials, cf. Section 2.2.1 and [15].

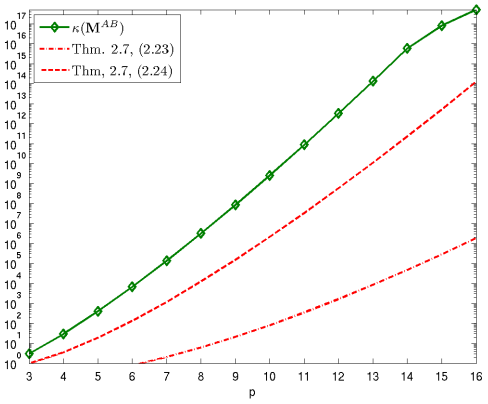

(a) $\kappa(\boldsymbol{M}^{AB})$ and lower bounds.

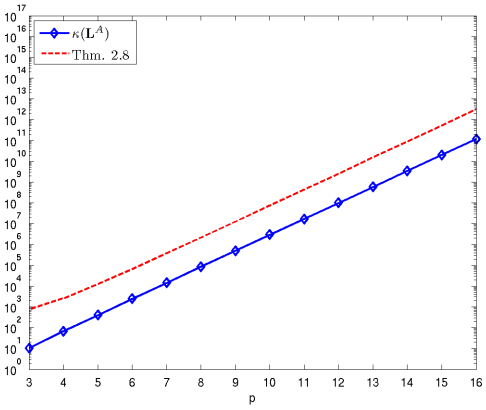

(b) $\kappa(\boldsymbol{L}^{A})$ and upper bounds

Figure 4.2: Condition number of the Vandermonde matrix $\boldsymbol{M}^{AB} \in \mathbb{C}^{p\times p}$, cf. Section 2.2.1 and [15], and the Lagrange matrix $\boldsymbol{L}^{A} \in \mathbb{C}^{p\times p}$, cf. Section 2.2.2, with respect to the local expansion degree p.

4.2 Accuracy of the Butterfly scheme

Regarding the accuracy of the whole algorithm, we draw coefficients $\hat{f}_k \in [-\frac{1}{2}, \frac{1}{2}] \times [-\frac{1}{2}, \frac{1}{2}]\mathrm{i}$, $k = 1, \dots, M_2$, at random from the uniform distribution and consider the relative error

$$\varepsilon_2 := \max_{j=1,\dots,M_1} \frac{|u(\boldsymbol{x}_j) - \tilde{u}(\boldsymbol{x}_j)|}{\|\hat{\boldsymbol{f}}\|_1} \leq 2d(L+1)c_0 c_1^{-p},$$

where $u, \tilde{u} : [0, N]^d \to \mathbb{C}$ denote the function to evaluate (3.1) and its approximation (3.4) and the upper bound is due to Corollary 3.2. We compare the quantity ε_2 and the upper

bound from Theorem 3.1 for the monomial and the Lagrange type realisation in Figure 4.3. In all four tests as well as further experiments for $d = 3$ and $d = 4$, the total error decays exponentially with p but is again limited for the mononial type realisation. In all cases, a least squares fit reveals a numerical error decay $\varepsilon_2 \approx C \cdot 16^{-p}$, where the constant C seems to depend neither on d nor L.

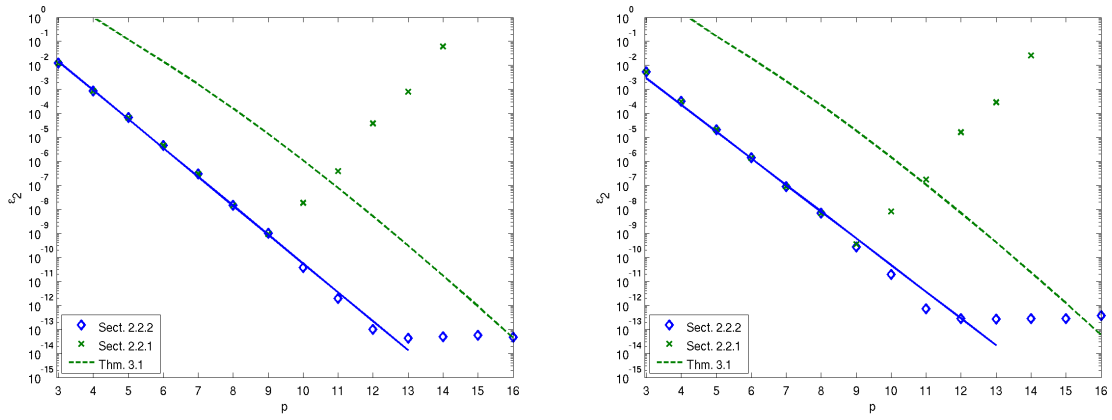

(a) $d = 1$, $N = 2^{10}$.

(b) $d = 1$, $N = 2^{14}$.

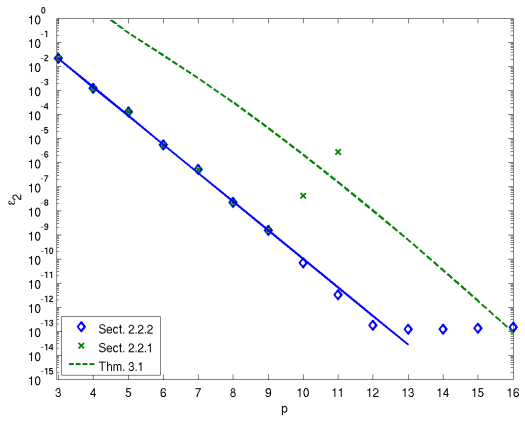

(c) $d = 2$, $N = 2^{10}$.

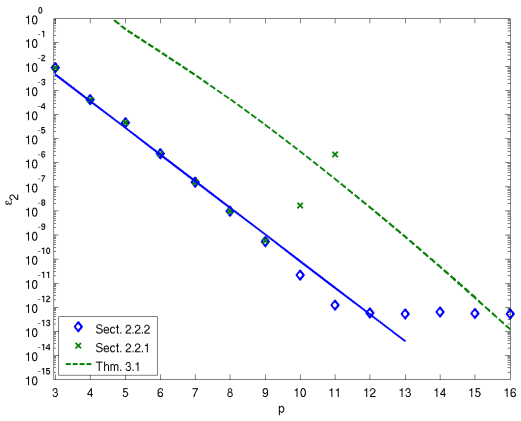

(d) $d = 2$, $N = 2^{14}$.

Figure 4.3: Relative error ε_2 with respect to the local expansion degree p for the realisation via Lagrange functions, cf. Section 2.2.2, and monomials, cf. Section 2.2.1.

Our second experiment touches the question whether the error really increases for increasing nonharmonic bandwidth as predicted by Corollary 3.2, i.e., $\varepsilon_2 \approx C_{p,d}L$. While randomly drawn coefficients $\hat{f}_k \in \mathbb{C}$, as in the previous test, did not show this increase, using constant coefficients $\hat{f}_k = 1$ indeed supports our findings in Figure 4.4.

4.3 Computational times

Finally, we compare the computational times, measured by the MATLAB functions `tic` and `toc`, of the naive evaluation (1.1) and Algorithm 1 for fixed spatial dimensions $d = 1, 2, 3, 4$,

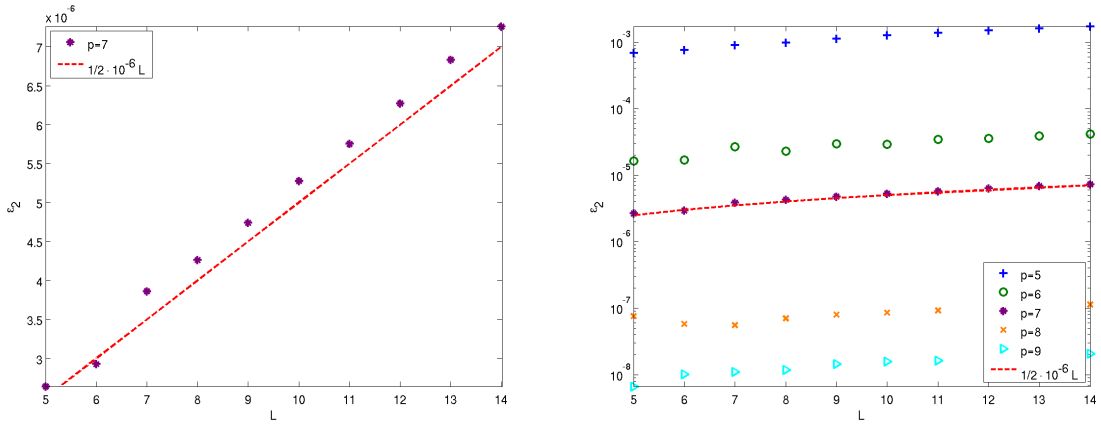

(a) $d = 1$, $\hat{f}_k = 1$

(b) Logarithmic scale.

Figure 4.4: Relative error ε_2 with respect to the nonharmonic bandwidth L.

fixed local expansion degrees $p = 4, 8$, and with respect to increasing nonharmonic bandwidth N. We draw coefficients $\hat{f}_k \in [-\frac{1}{2}, \frac{1}{2}] \times [-\frac{1}{2}, \frac{1}{2}]$i and source and target nodes $\boldsymbol{\xi}_k, \boldsymbol{x}_j \in [0, N]^d$, $k = 1, \ldots, M_2$, $j = 1, \ldots, M_1$, at random from the uniform distribution (on the submanifold). As discussed in Section 3.2, we consider three realisations of the interpolation operator, the monomial type basis, cf. Section 2.2.1, the Lagrange type basis, cf. Section 2.2.2, and the Lagrange type basis with precomputation of the Lagrange functions at the final evaluation nodes, denoted subsequently by Section 2.2.2*.

Figure 4.5 shows the measured times for $d = 1$ and $M_1 = M_2 = N$ sampling nodes in $\boldsymbol{\xi}_k, \boldsymbol{x}_j \in [0, N]$. The break even with the naive method occurs at $N = 32$ and we see some increase for a larger local expansion degree $p = 8$ when no precomputation is done. Figure 4.6 gives the results for $d = 2, 3, 4$ with $M_1 = M_2 = N^{d-1}$ sampling nodes on ellipses, spheres, and hyperplanes, respectively. Precomputation of the Lagrange functions in the last step of the algorithm does not gain any improvement here. Finally note that the break even with the naive algorithm occurs at a suitable problem size but a further reduction in absolute computing time is necessary for real applications.

5 Summary

Recently, the butterfly approximation scheme has been used for the development of a fast Fourier transform for sparse data [1, 15] which takes $\mathcal{O}(N^{d-1} \log N p^{d+1})$ floating point operations for $d \geq 2$, $M_1 = M_2 = \mathcal{O}(N^{d-1})$, and well distributed sampling sets $\tilde{T}, \tilde{X}$ on smooth $d-1$ dimensional manifolds, and a local expansion degree $p \in \mathbb{N}$.

We presented a rigorous error analysis of this algorithm, showing that the local expansion degree grows like $p \approx |\log \varepsilon| + \log \log N$ and thus gave a precise complexity estimate for the scheme. Moreover, we showed theoretically as well as numerically, that the original scheme becomes numerically unstable if a large local expansion degree is used and developed a stable variant by representing all approximations in a Lagrange type basis.

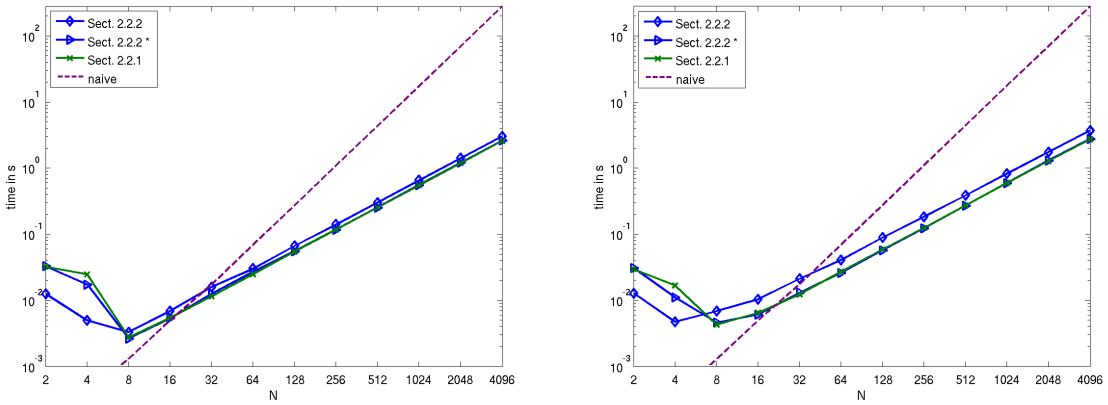

(a) $d = 1$, $p = 4$.

(b) $d = 1$, $p = 8$.

Figure 4.5: Computational time of the butterfly (nonsparse) FFT with respect to the non-harmonic bandwidth and problem size $N = M_1 = M_2$.

Acknowledgement

The authors gratefully acknowledge support by the German Research Foundation within the project KU 2557/1-1 and by the Helmholtz Association within the young investigator group VH-NG-526.

References

[1] A. Aydiner, W. C. Chew, J. Song, and T. J. Cui. A sparse data fast Fourier transform (SDFFT). *IEEE Trans. Antennas and Propagation*, 51(11):3161 – 3170, 2003.

[2] E. Candès, L. Demanet, and L. Ying. A fast butterfly algorithm for the computation of Fourier integral operators. *Multiscale Model. Simul.*, 7(4):1727–1750, 2009.

[3] P. Duhamel and M. Vetterli. Fast Fourier transforms: a tutorial review and a state of the art. *Signal Process.*, 19:259–299, 1990.

[4] A. Edelman, P. McCorquodale, and S. Toledo. The future fast Fourier transform? *SIAM J. Sci. Comput.*, 20(3):1094–1114, 1999.

[5] B. Elbel and G. Steidl. Fast Fourier transform for nonequispaced data. In C. K. Chui and L. L. Schumaker, editors, *Approximation Theory IX*, pages 39 – 46, Nashville, 1998. Vanderbilt University Press.

[6] T. Finck, G. Heinig, and K. Rost. An inversion formula and fast algorithms for Cauchy-Vandermonde matrices. *Linear Algebra Appl.*, 183:179–191, 1993.

[7] M. Frigo and S. G. Johnson. The design and implementation of FFTW3. *Proceedings of the* IEEE, 93:216 – 231, 2005.

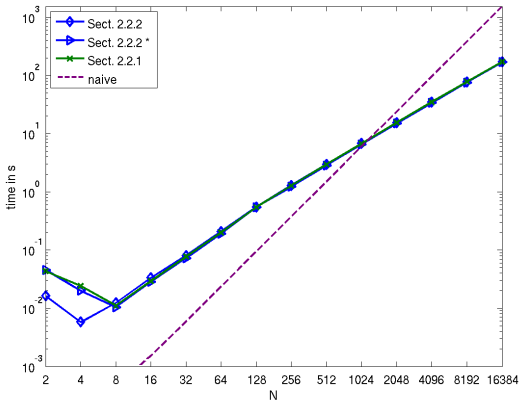

(a) $d = 2$, $p = 4$.

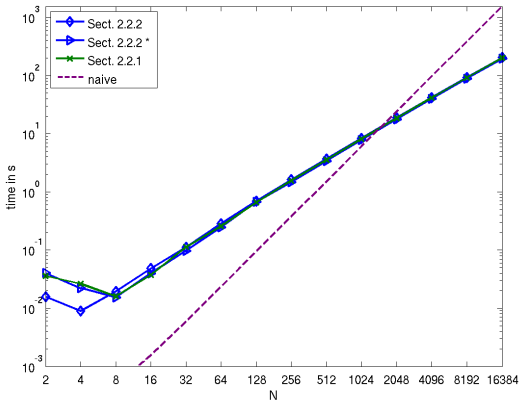

(b) $d = 2$, $p = 8$.

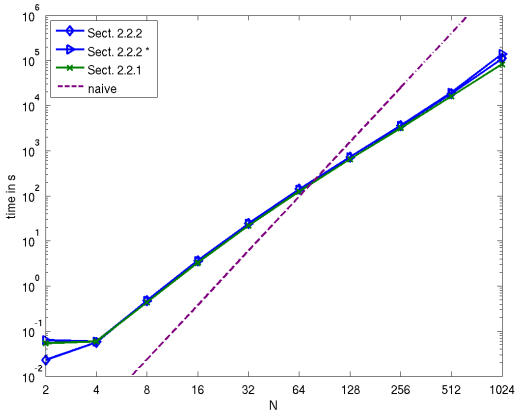

(c) $d = 3$, $p = 4$.

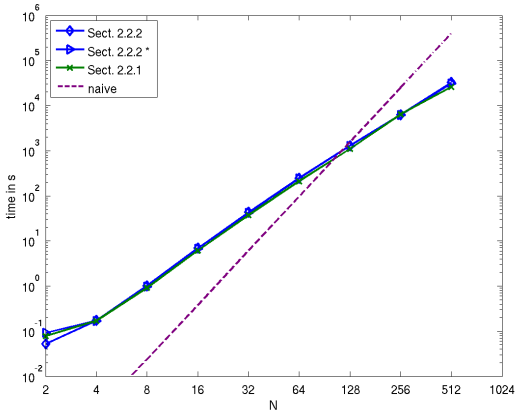

(d) $d = 3$, $p = 8$.

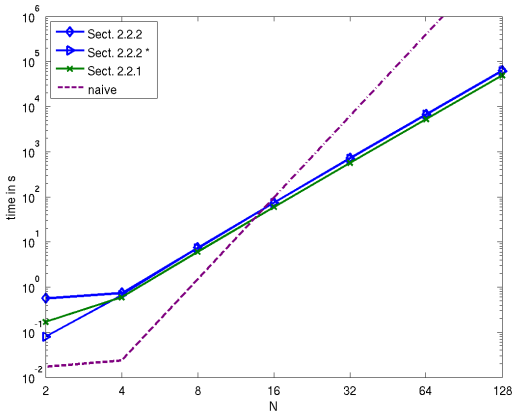

(e) $d = 4$, $p = 4$.

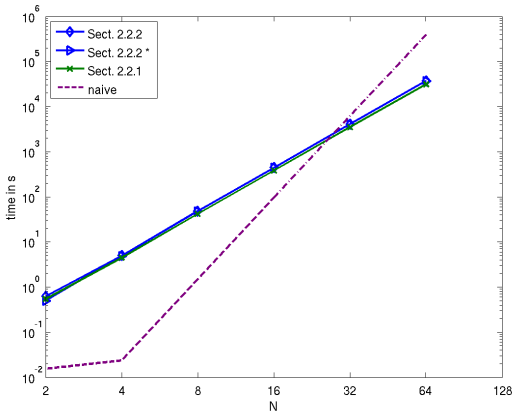

(f) $d = 4$, $p = 8$.

Figure 4.6: Computational time of the butterfly sparse FFT with respect to the nonharmonic bandwidth N and problem sizes $M_1 = M_2 = N^{d-1}$.

[8] L. Greengard and J.-Y. Lee. Accelerating the nonuniform fast Fourier transform. *SIAM Rev.*, 46:443 – 454, 2004.

[9] J. Keiner, S. Kunis, and D. Potts. Using NFFT3 - a software library for various nonequispaced fast Fourier transforms. *ACM Trans. Math. Software*, 36:Article 19, 1 – 30, 2009.

[10] T. G. Kolda and B. W. Bader. Tensor decompositions and applications. *SIAM Review*, 51(3):455–500, September 2009.

[11] E. Michielssen and A. Boag. A multilevel matrix decomposition algorithm for analyzing scattering from large structures. *IEEE Trans. Antennas and Propagation*, 44(8):1086 –1093, 1996.

[12] M. O'Neil, F. Woolfe, and V. Rokhlin. An algorithm for the rapid evaluation of special function transforms. *Appl. Comput. Harmon. Anal.*, 28(2):203–226, 2010.

[13] T. J. Rivlin. *Chebyshev polynomials*. Pure and Applied Mathematics (New York). John Wiley & Sons Inc., New York, second edition, 1990. From approximation theory to algebra and number theory.

[14] M. Tygert. Fast algorithms for spherical harmonic expansions, III. *J. Comput. Phys.*, 229(18):6181–6192, 2010.

[15] L. Ying. Sparse Fourier transform via butterfly algorithm. *SIAM J. Sci. Comput.*, 31(3):1678–1694, 2009.

[16] L. Ying and S. Fomel. Fast computation of partial Fourier transforms. *Multiscale Model. Simul.*, 8(1):110–124, 2009.

[17] R. M. Young. *An introduction to nonharmonic Fourier series*. Academic Press Inc., San Diego, CA, first edition, 2001.

Preprint Series DFG-SPP 1324

http://www.dfg-spp1324.de

Reports

[1] R. Ramlau, G. Teschke, and M. Zhariy. A Compressive Landweber Iteration for Solving Ill-Posed Inverse Problems. Preprint 1, DFG-SPP 1324, September 2008.

[2] G. Plonka. The Easy Path Wavelet Transform: A New Adaptive Wavelet Transform for Sparse Representation of Two-dimensional Data. Preprint 2, DFG-SPP 1324, September 2008.

[3] E. Novak and H. Woźniakowski. Optimal Order of Convergence and (In-) Tractability of Multivariate Approximation of Smooth Functions. Preprint 3, DFG-SPP 1324, October 2008.

[4] M. Espig, L. Grasedyck, and W. Hackbusch. Black Box Low Tensor Rank Approximation Using Fibre-Crosses. Preprint 4, DFG-SPP 1324, October 2008.

[5] T. Bonesky, S. Dahlke, P. Maass, and T. Raasch. Adaptive Wavelet Methods and Sparsity Reconstruction for Inverse Heat Conduction Problems. Preprint 5, DFG-SPP 1324, January 2009.

[6] E. Novak and H. Woźniakowski. Approximation of Infinitely Differentiable Multivariate Functions Is Intractable. Preprint 6, DFG-SPP 1324, January 2009.

[7] J. Ma and G. Plonka. A Review of Curvelets and Recent Applications. Preprint 7, DFG-SPP 1324, February 2009.

[8] L. Denis, D. A. Lorenz, and D. Trede. Greedy Solution of Ill-Posed Problems: Error Bounds and Exact Inversion. Preprint 8, DFG-SPP 1324, April 2009.

[9] U. Friedrich. A Two Parameter Generalization of Lions' Nonoverlapping Domain Decomposition Method for Linear Elliptic PDEs. Preprint 9, DFG-SPP 1324, April 2009.

[10] K. Bredies and D. A. Lorenz. Minimization of Non-smooth, Non-convex Functionals by Iterative Thresholding. Preprint 10, DFG-SPP 1324, April 2009.

[11] K. Bredies and D. A. Lorenz. Regularization with Non-convex Separable Constraints. Preprint 11, DFG-SPP 1324, April 2009.

[12] M. Döhler, S. Kunis, and D. Potts. Nonequispaced Hyperbolic Cross Fast Fourier Transform. Preprint 12, DFG-SPP 1324, April 2009.

[13] C. Bender. Dual Pricing of Multi-Exercise Options under Volume Constraints. Preprint 13, DFG-SPP 1324, April 2009.

[14] T. Müller-Gronbach and K. Ritter. Variable Subspace Sampling and Multi-level Algorithms. Preprint 14, DFG-SPP 1324, May 2009.

[15] G. Plonka, S. Tenorth, and A. Iske. Optimally Sparse Image Representation by the Easy Path Wavelet Transform. Preprint 15, DFG-SPP 1324, May 2009.

[16] S. Dahlke, E. Novak, and W. Sickel. Optimal Approximation of Elliptic Problems by Linear and Nonlinear Mappings IV: Errors in L_2 and Other Norms. Preprint 16, DFG-SPP 1324, June 2009.

[17] B. Jin, T. Khan, P. Maass, and M. Pidcock. Function Spaces and Optimal Currents in Impedance Tomography. Preprint 17, DFG-SPP 1324, June 2009.

[18] G. Plonka and J. Ma. Curvelet-Wavelet Regularized Split Bregman Iteration for Compressed Sensing. Preprint 18, DFG-SPP 1324, June 2009.

[19] G. Teschke and C. Borries. Accelerated Projected Steepest Descent Method for Nonlinear Inverse Problems with Sparsity Constraints. Preprint 19, DFG-SPP 1324, July 2009.

[20] L. Grasedyck. Hierarchical Singular Value Decomposition of Tensors. Preprint 20, DFG-SPP 1324, July 2009.

[21] D. Rudolf. Error Bounds for Computing the Expectation by Markov Chain Monte Carlo. Preprint 21, DFG-SPP 1324, July 2009.

[22] M. Hansen and W. Sickel. Best m-term Approximation and Lizorkin-Triebel Spaces. Preprint 22, DFG-SPP 1324, August 2009.

[23] F.J. Hickernell, T. Müller-Gronbach, B. Niu, and K. Ritter. Multi-level Monte Carlo Algorithms for Infinite-dimensional Integration on $\mathbb{R}^{\mathbb{N}}$. Preprint 23, DFG-SPP 1324, August 2009.

[24] S. Dereich and F. Heidenreich. A Multilevel Monte Carlo Algorithm for Lévy Driven Stochastic Differential Equations. Preprint 24, DFG-SPP 1324, August 2009.

[25] S. Dahlke, M. Fornasier, and T. Raasch. Multilevel Preconditioning for Adaptive Sparse Optimization. Preprint 25, DFG-SPP 1324, August 2009.

[26] S. Dereich. Multilevel Monte Carlo Algorithms for Lévy-driven SDEs with Gaussian Correction. Preprint 26, DFG-SPP 1324, August 2009.

[27] G. Plonka, S. Tenorth, and D. Roşca. A New Hybrid Method for Image Approximation using the Easy Path Wavelet Transform. Preprint 27, DFG-SPP 1324, October 2009.

[28] O. Koch and C. Lubich. Dynamical Low-rank Approximation of Tensors. Preprint 28, DFG-SPP 1324, November 2009.

[29] E. Faou, V. Gradinaru, and C. Lubich. Computing Semi-classical Quantum Dynamics with Hagedorn Wavepackets. Preprint 29, DFG-SPP 1324, November 2009.

[30] D. Conte and C. Lubich. An Error Analysis of the Multi-configuration Time-dependent Hartree Method of Quantum Dynamics. Preprint 30, DFG-SPP 1324, November 2009.

[31] C. E. Powell and E. Ullmann. Preconditioning Stochastic Galerkin Saddle Point Problems. Preprint 31, DFG-SPP 1324, November 2009.

[32] O. G. Ernst and E. Ullmann. Stochastic Galerkin Matrices. Preprint 32, DFG-SPP 1324, November 2009.

[33] F. Lindner and R. L. Schilling. Weak Order for the Discretization of the Stochastic Heat Equation Driven by Impulsive Noise. Preprint 33, DFG-SPP 1324, November 2009.

[34] L. Kämmerer and S. Kunis. On the Stability of the Hyperbolic Cross Discrete Fourier Transform. Preprint 34, DFG-SPP 1324, December 2009.

[35] P. Cerejeiras, M. Ferreira, U. Kähler, and G. Teschke. Inversion of the noisy Radon transform on $SO(3)$ by Gabor frames and sparse recovery principles. Preprint 35, DFG-SPP 1324, January 2010.

[36] T. Jahnke and T. Udrescu. Solving Chemical Master Equations by Adaptive Wavelet Compression. Preprint 36, DFG-SPP 1324, January 2010.

[37] P. Kittipoom, G. Kutyniok, and W.-Q Lim. Irregular Shearlet Frames: Geometry and Approximation Properties. Preprint 37, DFG-SPP 1324, February 2010.

[38] G. Kutyniok and W.-Q Lim. Compactly Supported Shearlets are Optimally Sparse. Preprint 38, DFG-SPP 1324, February 2010.

[39] M. Hansen and W. Sickel. Best m-Term Approximation and Tensor Products of Sobolev and Besov Spaces – the Case of Non-compact Embeddings. Preprint 39, DFG-SPP 1324, March 2010.

[40] B. Niu, F.J. Hickernell, T. Müller-Gronbach, and K. Ritter. Deterministic Multi-level Algorithms for Infinite-dimensional Integration on $\mathbb{R}^{\mathbb{N}}$. Preprint 40, DFG-SPP 1324, March 2010.

[41] P. Kittipoom, G. Kutyniok, and W.-Q Lim. Construction of Compactly Supported Shearlet Frames. Preprint 41, DFG-SPP 1324, March 2010.

[42] C. Bender and J. Steiner. Error Criteria for Numerical Solutions of Backward SDEs. Preprint 42, DFG-SPP 1324, April 2010.

[43] L. Grasedyck. Polynomial Approximation in Hierarchical Tucker Format by Vector-Tensorization. Preprint 43, DFG-SPP 1324, April 2010.

[44] M. Hansen und W. Sickel. Best m-Term Approximation and Sobolev-Besov Spaces of Dominating Mixed Smoothness - the Case of Compact Embeddings. Preprint 44, DFG-SPP 1324, April 2010.

[45] P. Binev, W. Dahmen, and P. Lamby. Fast High-Dimensional Approximation with Sparse Occupancy Trees. Preprint 45, DFG-SPP 1324, May 2010.

[46] J. Ballani and L. Grasedyck. A Projection Method to Solve Linear Systems in Tensor Format. Preprint 46, DFG-SPP 1324, May 2010.

[47] P. Binev, A. Cohen, W. Dahmen, R. DeVore, G. Petrova, and P. Wojtaszczyk. Convergence Rates for Greedy Algorithms in Reduced Basis Methods. Preprint 47, DFG-SPP 1324, May 2010.

[48] S. Kestler and K. Urban. Adaptive Wavelet Methods on Unbounded Domains. Preprint 48, DFG-SPP 1324, June 2010.

[49] H. Yserentant. The Mixed Regularity of Electronic Wave Functions Multiplied by Explicit Correlation Factors. Preprint 49, DFG-SPP 1324, June 2010.

[50] H. Yserentant. On the Complexity of the Electronic Schrödinger Equation. Preprint 50, DFG-SPP 1324, June 2010.

[51] M. Guillemard and A. Iske. Curvature Analysis of Frequency Modulated Manifolds in Dimensionality Reduction. Preprint 51, DFG-SPP 1324, June 2010.

[52] E. Herrholz and G. Teschke. Compressive Sensing Principles and Iterative Sparse Recovery for Inverse and Ill-Posed Problems. Preprint 52, DFG-SPP 1324, July 2010.

[53] L. Kämmerer, S. Kunis, and D. Potts. Interpolation Lattices for Hyperbolic Cross Trigonometric Polynomials. Preprint 53, DFG-SPP 1324, July 2010.

[54] G. Kutyniok and W.-Q Lim. Shearlets on Bounded Domains. Preprint 54, DFG-SPP 1324, July 2010.

[55] A. Zeiser. Wavelet Approximation in Weighted Sobolev Spaces of Mixed Order with Applications to the Electronic Schrödinger Equation. Preprint 55, DFG-SPP 1324, July 2010.

[56] G. Kutyniok, J. Lemvig, and W.-Q Lim. Compactly Supported Shearlets. Preprint 56, DFG-SPP 1324, July 2010.

[57] A. Zeiser. On the Optimality of the Inexact Inverse Iteration Coupled with Adaptive Finite Element Methods. Preprint 57, DFG-SPP 1324, July 2010.

[58] S. Jokar. Sparse Recovery and Kronecker Products. Preprint 58, DFG-SPP 1324, August 2010.

[59] T. Aboiyar, E. H. Georgoulis, and A. Iske. Adaptive ADER Methods Using Kernel-Based Polyharmonic Spline WENO Reconstruction. Preprint 59, DFG-SPP 1324, August 2010.

[60] O. G. Ernst, A. Mugler, H.-J. Starkloff, and E. Ullmann. On the Convergence of Generalized Polynomial Chaos Expansions. Preprint 60, DFG-SPP 1324, August 2010.

[61] S. Holtz, T. Rohwedder, and R. Schneider. On Manifolds of Tensors of Fixed TT-Rank. Preprint 61, DFG-SPP 1324, September 2010.

[62] J. Ballani, L. Grasedyck, and M. Kluge. Black Box Approximation of Tensors in Hierarchical Tucker Format. Preprint 62, DFG-SPP 1324, October 2010.

[63] M. Hansen. On Tensor Products of Quasi-Banach Spaces. Preprint 63, DFG-SPP 1324, October 2010.

[64] S. Dahlke, G. Steidl, and G. Teschke. Shearlet Coorbit Spaces: Compactly Supported Analyzing Shearlets, Traces and Embeddings. Preprint 64, DFG-SPP 1324, October 2010.

[65] W. Hackbusch. Tensorisation of Vectors and their Efficient Convolution. Preprint 65, DFG-SPP 1324, November 2010.

[66] P. A. Cioica, S. Dahlke, S. Kinzel, F. Lindner, T. Raasch, K. Ritter, and R. L. Schilling. Spatial Besov Regularity for Stochastic Partial Differential Equations on Lipschitz Domains. Preprint 66, DFG-SPP 1324, November 2010.

[67] E. Novak and H. Woźniakowski. On the Power of Function Values for the Approximation Problem in Various Settings. Preprint 67, DFG-SPP 1324, November 2010.

[68] A. Hinrichs, E. Novak, and H. Woźniakowski. The Curse of Dimensionality for Monotone and Convex Functions of Many Variables. Preprint 68, DFG-SPP 1324, November 2010.

[69] G. Kutyniok and W.-Q Lim. Image Separation Using Shearlets. Preprint 69, DFG-SPP 1324, November 2010.

[70] B. Jin and P. Maass. An Analysis of Electrical Impedance Tomography with Applications to Tikhonov Regularization. Preprint 70, DFG-SPP 1324, December 2010.

[71] S. Holtz, T. Rohwedder, and R. Schneider. The Alternating Linear Scheme for Tensor Optimisation in the TT Format. Preprint 71, DFG-SPP 1324, December 2010.

[72] T. Müller-Gronbach and K. Ritter. A Local Refinement Strategy for Constructive Quantization of Scalar SDEs. Preprint 72, DFG-SPP 1324, December 2010.

[73] T. Rohwedder and R. Schneider. An Analysis for the DIIS Acceleration Method used in Quantum Chemistry Calculations. Preprint 73, DFG-SPP 1324, December 2010.

[74] C. Bender and J. Steiner. Least-Squares Monte Carlo for Backward SDEs. Preprint 74, DFG-SPP 1324, December 2010.

[75] C. Bender. Primal and Dual Pricing of Multiple Exercise Options in Continuous Time. Preprint 75, DFG-SPP 1324, December 2010.

[76] H. Harbrecht, M. Peters, and R. Schneider. On the Low-rank Approximation by the Pivoted Cholesky Decomposition. Preprint 76, DFG-SPP 1324, December 2010.

[77] P. A. Cioica, S. Dahlke, N. Döhring, S. Kinzel, F. Lindner, T. Raasch, K. Ritter, and R. L. Schilling. Adaptive Wavelet Methods for Elliptic Stochastic Partial Differential Equations. Preprint 77, DFG-SPP 1324, January 2011.

[78] G. Plonka, S. Tenorth, and A. Iske. Optimal Representation of Piecewise Hölder Smooth Bivariate Functions by the Easy Path Wavelet Transform. Preprint 78, DFG-SPP 1324, January 2011.

[79] A. Mugler and H.-J. Starkloff. On Elliptic Partial Differential Equations with Random Coefficients. Preprint 79, DFG-SPP 1324, January 2011.

[80] T. Müller-Gronbach, K. Ritter, and L. Yaroslavtseva. A Derandomization of the Euler Scheme for Scalar Stochastic Differential Equations. Preprint 80, DFG-SPP 1324, January 2011.

[81] W. Dahmen, C. Huang, C. Schwab, and G. Welper. Adaptive Petrov-Galerkin methods for first order transport equations. Preprint 81, DFG-SPP 1324, January 2011.

[82] K. Grella and C. Schwab. Sparse Tensor Spherical Harmonics Approximation in Radiative Transfer. Preprint 82, DFG-SPP 1324, January 2011.

[83] D.A. Lorenz, S. Schiffler, and D. Trede. Beyond Convergence Rates: Exact Inversion With Tikhonov Regularization With Sparsity Constraints. Preprint 83, DFG-SPP 1324, January 2011.

[84] S. Dereich, M. Scheutzow, and R. Schottstedt. Constructive quantization: Approximation by empirical measures. Preprint 84, DFG-SPP 1324, January 2011.

[85] S. Dahlke and W. Sickel. On Besov Regularity of Solutions to Nonlinear Elliptic Partial Differential Equations. Preprint 85, DFG-SPP 1324, January 2011.

[86] S. Dahlke, U. Friedrich, P. Maass, T. Raasch, and R.A. Ressel. An adaptive wavelet method for parameter identification problems in parabolic partial differential equations. Preprint 86, DFG-SPP 1324, January 2011.

[87] A. Cohen, W. Dahmen, and G. Welper. Adaptivity and Variational Stabilization for Convection-Diffusion Equations. Preprint 87, DFG-SPP 1324, January 2011.

[88] T. Jahnke. On Reduced Models for the Chemical Master Equation. Preprint 88, DFG-SPP 1324, January 2011.

[89] P. Binev, W. Dahmen, R. DeVore, P. Lamby, D. Savu, and R. Sharpley. Compressed Sensing and Electron Microscopy. Preprint 89, DFG-SPP 1324, March 2011.

[90] P. Binev, F. Blanco-Silva, D. Blom, W. Dahmen, P. Lamby, R. Sharpley, and T. Vogt. High Quality Image Formation by Nonlocal Means Applied to High-Angle Annular Dark Field Scanning Transmission Electron Microscopy (HAADF-STEM). Preprint 90, DFG-SPP 1324, March 2011.

[91] R. A. Ressel. A Parameter Identification Problem for a Nonlinear Parabolic Differential Equation. Preprint 91, DFG-SPP 1324, May 2011.

[92] G. Kutyniok. Data Separation by Sparse Representations. Preprint 92, DFG-SPP 1324, May 2011.

[93] M. A. Davenport, M. F. Duarte, Y. C. Eldar, and G. Kutyniok. Introduction to Compressed Sensing. Preprint 93, DFG-SPP 1324, May 2011.

[94] H.-C. Kreusler and H. Yserentant. The Mixed Regularity of Electronic Wave Functions in Fractional Order and Weighted Sobolev Spaces. Preprint 94, DFG-SPP 1324, June 2011.

[95] E. Ullmann, H. C. Elman, and O. G. Ernst. Efficient Iterative Solvers for Stochastic Galerkin Discretizations of Log-Transformed Random Diffusion Problems. Preprint 95, DFG-SPP 1324, June 2011.

[96] S. Kunis and I. Melzer. On the Butterfly Sparse Fourier Transform. Preprint 96, DFG-SPP 1324, June 2011.